

<https://doi.org/10.3799/dqkx.2022.335>



# 越南昆嵩地体三叠纪花岗岩岩石成因及其特提斯构造意义

李慧玲<sup>1</sup>, 钱 鑫<sup>1,2\*</sup>, 余小清<sup>1</sup>, Pham Trung Hieu<sup>3</sup>, 张菲菲<sup>4</sup>, 余永琪<sup>1</sup>, 徐 畅<sup>1</sup>, 王岳军<sup>1,2</sup>

1. 中山大学地球科学与工程学院, 广东省地球动力作用与地质灾害重点实验室, 广东珠海 519082
2. 南方海洋科学与工程广东省实验室(珠海), 广东珠海 519082
3. 越南国立大学地质系, 越南胡志明市 70000
4. 西北大学地质学系, 陕西西安 710069

**摘要:** 昆嵩地体位于印支陆块的核部, 记录了大量的印支期岩浆作用和构造热事件, 是了解古特提斯洋演化及印支与华南陆块碰撞拼合过程的关键区域, 但目前对该期岩浆事件的成因及其与北部长山带的关系未能得到有效厘定。对昆嵩地体绥安(Huynh Tuy An)和胶寮(Chu Loan)地区的 Van Canh 花岗岩开展了岩相学、锆石 U-Pb 年代学、锆石原位 Hf 同位素和全岩地球化学分析, 以限定其形成时代、岩石成因及构造环境。锆石 U-Pb 定年显示花岗岩样品的结晶年龄为 244~239 Ma。该套样品包括了二长花岗岩和钾长花岗岩, 均属于高钾钙碱性系列。它们的 A/CNK 值为 1.03~1.21, 为 S 型花岗岩。花岗岩均显示明显的 Rb、Th 和 U 富集, 以及 Nb、Sr、Zr 和 Ti 的亏损, 并具有强烈的 Eu 负异常 ( $\text{Eu}/\text{Eu}^* = 0.24 \sim 0.56$ )。锆石具有富集的原位 Hf 同位素组成 ( $\epsilon_{\text{Hf}}(t) = -11.2 \sim -0.7$ ) 以及古—中元古代的 Hf 二阶模式年龄 ( $T_{\text{DM2}} = 1.98 \sim 1.31 \text{ Ga}$ )。研究表明该套中三叠世花岗岩是古元古代—中元古代变沉积岩部分熔融的产物, 并伴有少量变火成岩的加入。研究结合区域地质资料表明昆嵩地体中三叠世 Van Canh 花岗岩的成因与马江古特提斯分支洋闭合之后的印支与华南陆块的碰撞拼合有关, 形成于后碰撞阶段, 进而证实了长山带向南可以延伸至昆嵩地体内部。

**关键词:** 印支陆块; 越南昆嵩地体; 中三叠世; S型花岗岩; 古特提斯洋; 后碰撞; 地球化学。

中图分类号: P597

文章编号: 1000-2383(2023)04-1441-20

收稿日期: 2022-07-12

## Petrogenesis of Triassic Granites from Kontum Massif in Vietnam and Its Tethyan Tectonic Implications

Li Huiling<sup>1</sup>, Qian Xin<sup>1,2\*</sup>, Yu Xiaoqing<sup>1</sup>, Pham Trung Hieu<sup>3</sup>, Zhang Feifei<sup>4</sup>, Yu Yongqi<sup>1</sup>, Xu Chang<sup>1</sup>, Wang Yuejun<sup>1,2</sup>

1. Guangdong Key Laboratory of Geodynamics and Geohazards, School of Earth Sciences and Engineering, Sun Yat-sen University, Zhuhai 519082, China
2. Southern Marine Science and Engineering Guangdong Laboratory, Zhuhai 519082, China
3. Faculty of Geology, Vietnam National University, Ho Chi Minh 70000, Vietnam
4. Department of Geology, Northwest University, Xi'an 710069, China

**基金项目:** 国家自然科学基金项目(Nos. 41830211, 42072256); 广东省基础与应用基础研究基金项目(Nos. 2018B030312007, 2019B1515120019); 中山大学高校基本业务费(No. 22lgqb14)

**作者简介:** 李慧玲(1998—), 女, 硕士研究生, 地球化学专业。ORCID: 0000-0002-3590-1197. E-mail: lihling33@mail2.sysu.edu.cn

\*通讯作者: 钱鑫, ORCID: 0000-0002-3587-861X. E-mail: qianx3@mail.sysu.edu.cn

**引用格式:** 李慧玲, 钱鑫, 余小清, Pham Trung Hieu, 张菲菲, 余永琪, 徐畅, 王岳军, 2023. 越南昆嵩地体三叠纪花岗岩岩石成因及其特提斯构造意义. 地球科学, 48(4): 1441—1460.

**Citation:** Li Huiling, Qian Xin, Yu Xiaoqing, Pham Trung Hieu, Zhang Feifei, Yu Yongqi, Xu Chang, Wang Yuejun, 2023. Petrogenesis of Triassic Granites from Kontum Massif in Vietnam and Its Tethyan Tectonic Implications. *Earth Science*, 48(4): 1441—1460.

**Abstract:** Kontum massif in the central Indochina records abundant Indosinian magmatism and tectonic thermal events, and is a key area for investigating the tectonic evolution of Paleotethyan ocean and subsequent collision between the Indochina and South China blocks. However, the origin of this Indosinian magmatism and its relationship with the Truong Son zone in the north are poorly constrained. In this study, it presents a set of petrographic, zircon U-Pb geochronological, zircon in-situ Hf isotopic, and whole-rock geochemical data for the granites from the Huyen Tuy An and Chu Loan area in the Kontum massif to constrain their crystallization ages, petrogenesis, and tectonic setting. Zircon U-Pb dating shows that the granites formed at 244–239 Ma. These samples contain monzogranites and K-feldspar granites and belong to the high-K calc-alkaline series. They are S-type granites with A/CNK values ranging from 1.03 to 1.21. These samples show enrichment of Rb, Th, and U, and depletion of Nb, Sr, Zr, and Ti, with obvious negative Eu anomalies ( $\text{Eu}/\text{Eu}^* = 0.24–0.56$ ). Their negative zircon  $\epsilon_{\text{Hf}}(t)$  values ( $(-11.2)–(-0.7)$ ) and Paleo- to Meso-Proterozoic Hf model ages ( $T_{\text{DM2}} = 1.98–1.31 \text{ Ga}$ ) indicate that these granites were derived from the partial melting of the Paleo- to Meso-Proterozoic metasedimentary rocks with a small amount of metaigneous component. Our new data along with the regional geological observations suggest that the Middle Triassic Van Canh granites in the Kontum massif were formed in a post-collisional setting in response to the collision between the Indochina and South China blocks following the closure of Song-Ma Paleotethyan branch. Our studies further suggest that the Truong Son zone can southerly extend to the central Kontum massif.

**Key words:** Indochina block; Kontum massif; Middle Triassic; S-type granite; Paleotethyan ocean; post-collision; geochemistry.

## 0 引言

古特提斯洋是晚古生代至早中生代存在于东南亚陆块群和东基梅里大陆之间的古大洋,该洋西起欧洲阿尔卑斯山脉,经中亚、西藏及我国西南部,进而延伸至东南亚等地(Bullard *et al.*, 1965; Acharyya, 1998; Metcalfe, 1998, 2006, 2011, 2013, 2017, 2021; Wakita and Metcalfe, 2005; Wang *et al.*, 2018; 栾锡武等, 2021; 钱鑫等, 2022)。随着古特提斯洋的俯冲闭合,一系列由冈瓦纳北缘分离的陆块(华南、印支、滇缅马和思茅等)与欧亚大陆东南缘发生碰撞拼合进而形成了中南半岛。目前在中南半岛已识别出多个古特提斯缝合带/构造带,包括了清迈—清莱古特提斯主缝合带、哀牢山—马江古特提斯分支洋缝合带、黎府—碧差汶、长山带、琅勃拉邦和景洪—难河—程逸—沙缴带等(图1a, Metcalfe, 1996, 2021; Sone and Metcalfe, 2008; Yang *et al.*, 2016; Zhao *et al.*, 2016; Qian *et al.*, 2016a, 2016b, 2016c, 2019; Wang *et al.*, 2016b, 2018, 2020; 赵国锋等, 2018; Zhang *et al.*, 2020; 吴松洋等, 2022)。其中,马江带被认为是印支与华南的缝合边界,其系统记录了三叠纪时期的俯冲—闭合演化历史(Chung *et al.*, 1997; Sone and Metcalfe, 2008; Jian *et al.*, 2009; Zi *et al.*, 2012a, 2012b; Zhang *et al.*, 2014, 2020; Wang *et al.*, 2018)。此外,长山带主体沿中南半岛东北部延伸,其北界为越南北部的马江带,南界为昆嵩地体北部的三岐—福山带,绵延约1000 km,构成了印支陆块北部最大的

构造岩浆岩带(图1a)。已有的研究证实了长山带内保存了晚古生代—早中生代与马江古特提斯分支洋的俯冲—闭合及随后的印支与华南陆块碰撞拼合有关的岩浆—沉积记录(Lepvrier *et al.*, 2008, 2011; Liu *et al.*, 2012; Hieu *et al.*, 2012, 2020; Wang *et al.*, 2016a; van Thanh *et al.*, 2019; Qian *et al.*, 2019; 钱鑫等, 2022)。

越南中部的昆嵩地体被认为是印支陆块的古老基底,已报道的年代学数据也显示该地体存在前寒武纪角闪岩相—麻粒岩相变质基底(Le Van De, 1997; 李兴振等, 2004; Tri and Khuc, 2011; 施美凤等, 2011; Zhang *et al.*, 2019)。此外,该地体还保存了加里东期(奥陶纪—志留纪)和印支期(二叠纪—三叠纪)的岩浆与变质作用,其中加里东期岩浆—变质事件被认为与原特提斯洋的演化有关(如Usuki *et al.*, 2009; Shi *et al.*, 2015; Hieu *et al.*, 2016; Owada *et al.*, 2016; Nguyen *et al.*, 2019; Minh *et al.*, 2020; Jiang *et al.*, 2020; Wang *et al.*, 2020, 2021; Trong *et al.*, 2021; Nakano *et al.*, 2021)。但是对印支期的岩浆作用及变质事件则存在不同的认识,包括了地幔柱成因(Owada *et al.*, 2007, 2016, 2020; Osanai *et al.*, 2008; Faure *et al.*, 2018)和古特提斯洋俯冲—闭合及之后的碰撞造山成因(Carter *et al.*, 2001; Lepvrier *et al.*, 2004, 2008; Hoa *et al.*, 2008, 2016; Usuki *et al.*, 2009; Sang, 2011; Nakano *et al.*, 2013, 2021; Hieu *et al.*, 2013, 2015, 2017, 2020; van Thanh *et al.*,

2019; Hung *et al.*, 2022).此外,已有的研究也主要集中在有限的年代学资料和沉积研究上(Nagy *et al.*, 2001; Hoa *et al.*, 2008; Nakano *et al.*, 2013; Hieu *et al.*, 2015; Kawaguchi *et al.*, 2021).因此,昆嵩地体二叠纪—三叠纪长英质火成岩的形成时代、岩石成因及与长山带的关系等均未能得到有效限定。

针对上述问题,作者在越南中部的昆嵩地区开展了系统的野外调查,并在绥安和胶寮地区识别出了一套保存完好的花岗岩岩体(图1b).针对这些花岗岩岩体,本文开展了系统的岩相学、锆石U-Pb年代学、锆石Lu-Hf同位素以及全岩地球化学分析,并结合区域同期长英质火成岩数据及相关地质资料,为昆嵩地体内古特提斯岩浆作用及构造演化提供新的约束。

## 1 地质概况与岩相学特征

印支陆块东部与华南陆块的交界为哀牢山—马江带,其西部则以景洪—难河—程逸—沙缴缝合

带为界与临沧—素可泰—庄他武里地体分开(图1a).越南中部的昆嵩地体位于印支陆块东部,其北以原特提斯三岐—福山带为界与长山带所分离,南与大叻带相连.该地体主要由前寒武纪结晶基底及盖层组成(Hutchison, 1989; Le Van De, 1997; 李兴振等, 2004),包括了太古宙和元古宙岩石单元,其中太古宙岩石可分为下、中、上三部分,下部为变基性火成岩和镁铁质麻粒岩,中部为具镁铁质至硅铝质过渡特征的斜长片麻岩,上部为硅铝质花岗质岩石.元古宙岩石由斜长片麻岩、辉长岩、角闪岩、矽线石片岩和混合岩组成(Le Van De, 1997; 李兴振等, 2004; 施美凤等, 2011).昆嵩地体的盖层主要由中三叠统、中侏罗统和白垩系沉积岩组成,其中中三叠统主要由碎屑岩、碳酸盐岩、砂砾岩和页岩组成,中侏罗统为磨拉石相砂砾岩层,白垩系为红层、泥灰岩、粉砂页岩和含膏岩层等(如Le Van De, 1997; 李兴振等, 2004; 王宏等, 2015; Xu *et al.*, 2022).此外,昆嵩地体内还存在3个主要的变质杂岩体(图1b),根据变质等级的不同分为麻粒岩相Kannak岩体、角闪岩相Ngoc Linh岩体和绿片岩相

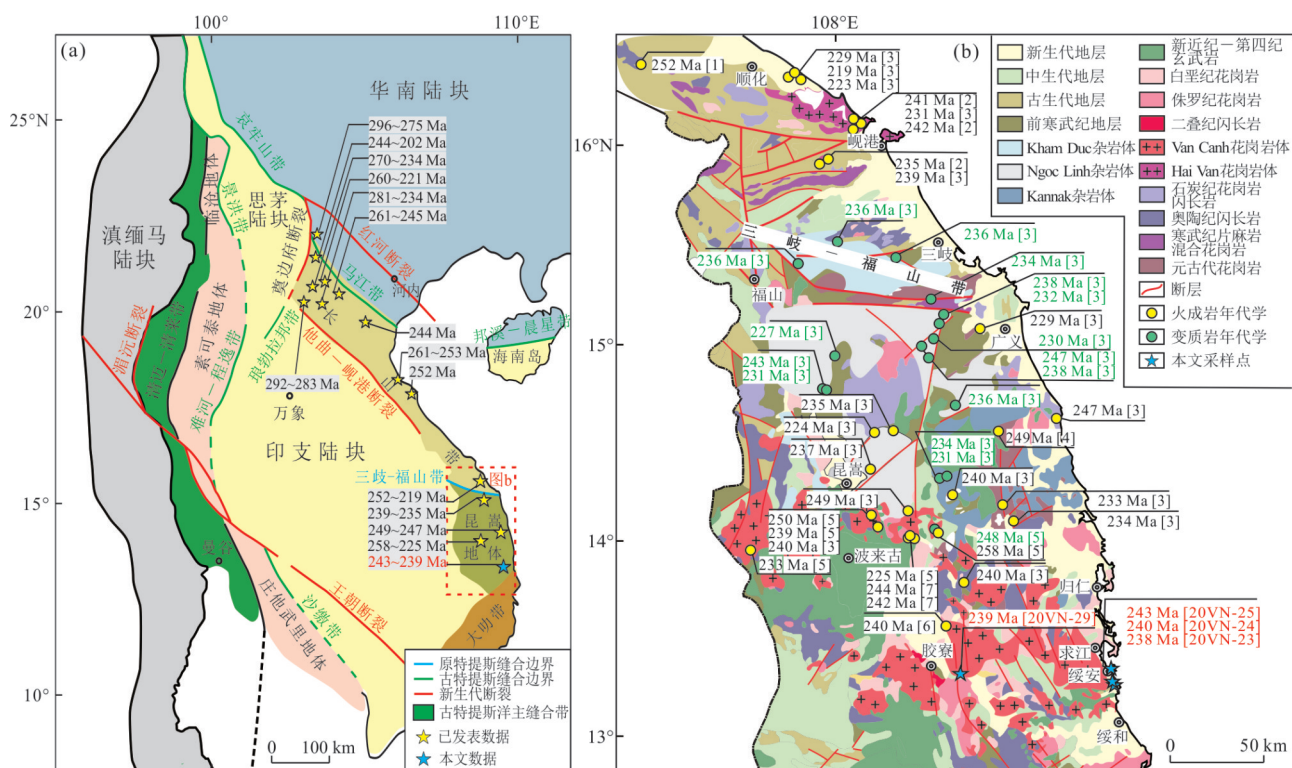


图1 东南亚地区构造划分简图(a)和研究区地质简图及长山带和昆嵩地体二叠纪—三叠纪岩浆岩与变质岩年龄分布(b)  
Fig. 1 Tectonic sketch map of SE Asia (a) and simplified geological map of the study area and the distribution of the Permian-Triassic felsic and metamorphic rocks in the Truong Son zone and Kontum massif (b)

图a据Sone and Metcalfe (2008); Wang *et al.* (2018); Qian *et al.* (2020); 图b年龄数据来源:[1] Shi *et al.* (2015); [2] Hieu *et al.* (2015); [3] Nakano *et al.* (2013); [4] Nagy *et al.* (2001); [5] Carter *et al.* (2001); [6] Hung *et al.* (2022); [7] Cuong *et al.* (2021)

Kham Duc 岩体. 变质岩和花岗岩的独居石 U-Th-Pb 定年结果显示该地体的变质杂岩主要受到 460~430 Ma 和 245~230 Ma 两期构造热事件的影响, 而花岗岩的侵位年龄则主要集中于 240~220 Ma, 为中一晚三叠世(Nakano *et al.*, 2013).

昆嵩地体发育了奥陶纪—志留纪(Thanh *et al.*, 2014; Hieu *et al.*, 2016; Minh *et al.*, 2020)、二叠纪—三叠纪(Nagy *et al.*, 2001; Hoa *et al.*, 2008; Nakano *et al.*, 2013; Hieu *et al.*, 2015)和白垩纪(Nguyen *et al.*, 2004; Shellnutt *et al.*, 2013)三期长英质岩浆作用. 其中奥陶纪—志留纪主要有 Chu Lai 花岗岩(454~445 Ma, 如 Thanh *et al.*, 2014)、Dai Loc 花岗岩(426~423 Ma, 如 Hieu *et al.*, 2016)、Kan Nack 片麻岩和 Ngoc Linh 片麻岩(450~422 Ma 和 462~429 Ma, Nakano *et al.*, 2013). 这些花岗质岩石主要以 I型和 S型为特征, 表现出与俯冲或碰撞相关的地球化学特征. 二叠纪—三叠纪主要以 Kan Nack 紫苏花岗岩和片麻岩(249 Ma 和 248~230 Ma, Nagy *et al.*, 2001; Nakano *et al.*, 2013)、Van Canh 花岗岩(251~229 Ma, 如 Hung *et al.*, 2022)、Kham Duc 片麻岩(236 Ma, 如 Nakano *et al.*, 2013)和 Ngoc Linh 片麻岩(251~230 Ma, Nakano *et al.*, 2013)为代表, 并被认为与地幔柱或印支与华南陆块的碰撞有关(Nagy *et al.*, 2001; Owada *et al.*, 2007, 2016, 2020; Osanai *et al.*, 2008; Hieu *et al.*, 2015; Hung *et al.*, 2022). 白垩纪花岗岩主要零星分布在昆嵩地体的南部地区, 并被认为与古太平洋的演化有关(Nguyen *et al.*, 2004; Shellnutt *et al.*, 2013).

昆嵩地体北部的 Hai Van 花岗岩体主要由含堇青石的花岗岩、黑云母花岗岩、花岗闪长岩、二云母花岗岩和细晶花岗岩组成, 年龄为 242~224 Ma, 被认为是长山带最南部的岩体(图 1b; 如 Thuc and Trung, 1995; Nakano *et al.*, 2013; Hieu *et al.*, 2015; van Thanh *et al.*, 2019). 三叠纪 Van Canh 花岗岩体是昆嵩地体最大的花岗岩体, 主要呈北西—南东向分布在地体的南部, 总面积超过 2 000 km<sup>2</sup>, 由 Van Canh、Hoa Lac、Tra Buon、Chu Loan、Kong Choro 等多个次级岩体组成(图 1b; Hung *et al.*, 2022). Van Canh 花岗岩主要侵入前寒武纪变质岩系, 并被侏罗纪沉积物不整合覆盖(Thuc and Trung, 1995; Tri and Khuc, 2011). 最近的研究表明 Van Canh 花岗岩锆石年龄为 251~229 Ma(图

1b; Cuong *et al.*, 2021; Hung *et al.*, 2022).

本文样品采自昆嵩地体南部的 Van Canh 花岗岩体(图 1b), 其中 20VN-23 采样点(109°17'46"E, 13°15'43"N)距绥和北部约 18 km, 位于 Chua Long Hai Tuy An Phu Yen 寺庙南 1 km 公路旁; 20VN-24 采样点(109°17'35"E, 13°16'31"N)距绥和北部约 20 km, 位于 Chua Long Hai Tuy An Phu Yen 寺庙北 0.5 km 公路旁; 样品 20VN-29 (108°32'52"E, 13°20'22"N)采自胶寮东约 15 km 的 QL25 公路旁. 这 3 个点位的样品均为块状构造的二长花岗岩, 表面风化较为严重, 风化面破碎呈土褐色, 选取灰白色新鲜面采集样品. 此外, 样品 20VN-25 (109°17'37"E, 13°21'14"N) 采自距绥和北部约 35 km 的 Ganh Da Dia 海湾内, 为肉红色块状构造的钾长花岗岩, 可见新生代玄武岩覆盖于花岗岩之上(图 2e). 镜下薄片观察表明二长花岗岩样品为细粒花岗结构, 矿物粒径为 0.2~2.0 mm, 主要矿物为石英(35%~40%)、碱性长石(~30%)、斜长石(20%~30%), 含有少量黑云母(~5%)、白云母(~3%)与绿帘石(~3%)等. 其中, 黑云母至斜长石、碱性长石、石英的矿物颗粒自形程度依次降低, 黑云母为半自形—自形, 斜长石自形程度高于钾长石和石英, 石英为他形. 两种长石含量相近, 碱性长石主要为条纹长石和正长石, 具条纹结构及卡斯巴双晶, 表面土化呈土黄褐色, 斜长石发育聚片双晶, 部分斜长石可见绢云母化(图 2b, 2d, 2f, 2h). 样品中还可见少量锂云母(<1%), 其呈片状分布于钾长石边缘(图 2b). 钾长花岗岩样品(20VN-29)为肉红色, 具细粒花岗结构, 矿物粒径在 0.1~0.3 mm 之间, 矿物组成为石英(~40%)、钾长石(~38%)、斜长石(~17%)以及少量黑云母(2%~5%)和绿帘石(<1%)(图 2h).

## 2 分析方法

### 2.1 锆石 U-Pb 定年及原位 Lu-Hf 同位素测定

本文研究样品在河北省廊坊市地质测绘院实验室通过磁选法和重液法进行锆石颗粒分选后制靶. 锆石的阴极发光图像(CL 图)在广州拓岩检测技术有限公司利用 TESCAN MIRA3 场发射扫描电子显微镜完成, 使用扫描电压为 10 kV、束流为 15 nA、放大倍率为 300~500 倍. 锆石 U-Pb 同位素定年在中山大学广东省地球动力作用与地质灾害重点实验室使用激光剥蚀系统与电感耦合等离子体质谱仪联用(LA-ICP-MS)完成. 实验中使用的

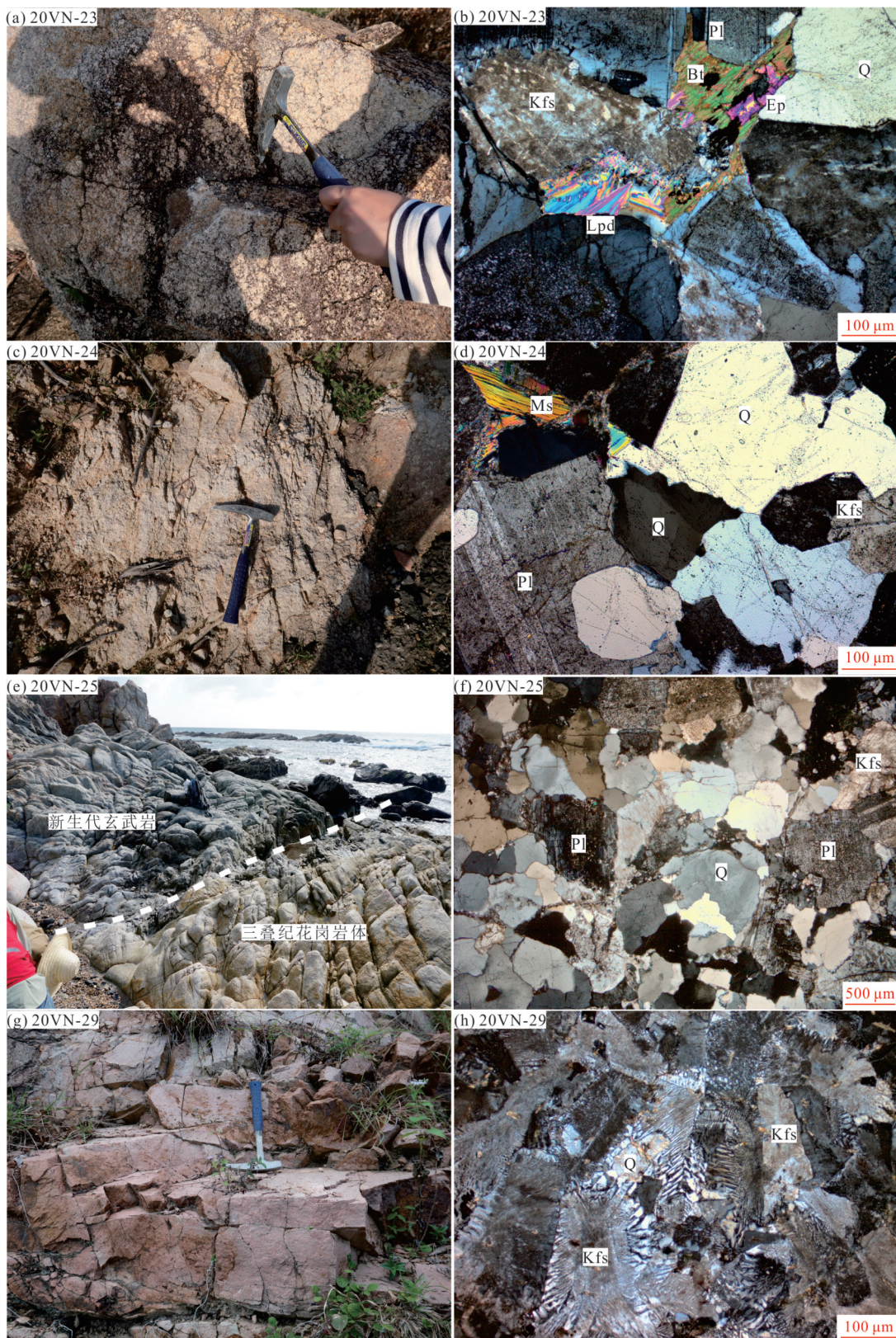


图2 昆嵩地体南部三叠纪 Van Canh 花岗岩野外露头和显微岩相学特征

Fig. 2 Field photos and photomicrographs of the Triassic Van Canh granites in southern Kontum massif  
 a~f. 二长花岗岩 (20VN-23, 20VN-24 和 20VN-25); g, h. 钾长花岗岩 (20VN-29). 矿物缩写: Q. 石英; Pl. 斜长石; Kfs. 钾长石; Bt. 黑云母; Ms. 白云母; Ep. 绿帘石; Lpd. 锂云母

激光束斑直径为  $32 \mu\text{m}$ , 激光脉冲频率为 5 Hz, 详细的分析测试过程见 Wang *et al.* (2020). 采用标准锆石 91500 ( $1062.4 \pm 0.6$  Ma; Wiedenbeck *et al.*, 1995) 用于 U-Pb 同位素分馏校正, 玻璃标准物质 NIST 610 用于微量元素校正. 利用 Glitter4.4.5 (Griffin *et al.*, 2008) 对原始数据进行处理, 使用 ISOPLOT 软件进行锆石 U-Pb 年龄谱和图的绘制以及加权平均年龄的计算 (Ludwig, 2003). 标样 91500 的分析结果介于  $1060 \sim 1066$  Ma, 与国际标准值 ( $1062.4$  Ma, Wiedenbeck *et al.*, 1995) 的方差和标准差分别为 1.85 和 1.36, 其离散程度小, 表明仪器状态稳定.

锆石原位 Lu-Hf 同位素分析在中山大学广东省地球动力作用与地质灾害重点实验室完成. 通过 Geolas HD 准分子 ArF 激光剥蚀系统和 Neptune Plus 多接收电感耦合等离子体质谱仪 (MC-ICP-MS) 联用完成测试, 详细分析流程类似于 Hu *et al.* (2012). 标样为 91500 和 Plešovice, 激光斑束直径和激光频率分别为  $44 \mu\text{m}$  和 8 Hz. 计算 Hf 初始同位素值选用  $1.867 \times 10^{-11} \text{ a}^{-1}$  的  $^{176}\text{Lu}$  衰变常数 (如 Söderlund *et al.*, 2004), 计算相对于亏损地幔的 Hf 模式年龄 ( $T_{\text{DM}}$ ) 使用  $^{176}\text{Hf}/^{177}\text{Hf} = 0.282772$  和  $^{176}\text{Lu}/^{177}\text{Hf} = 0.0332$  (如 Blichert-Toft and Albarède, 1997), 用大陆地壳平均值  $^{176}\text{Lu}/^{177}\text{Hf} = 0.015$  和  $f_{\text{cc}} = -0.55$  (Griffin *et al.*, 2002) 计算 Hf 的二阶模式年龄 ( $T_{\text{DM2}}$ ).

## 2.2 全岩主、微量元素分析

选用新鲜样品无污染粉碎至 200 目, 在中山大

学广东省地球动力作用与地质灾害重点实验室完成全岩主量和微量元素测定. 全岩主量元素分析使用 ARL Perform' X 4200 型 X 射线荧光光谱仪 (XRF), 采用熔片法制备样品, 称量烘干的样品与硼酸锂混合溶剂于坩埚中, 加入饱和的碘化铵 ( $\text{NH}_4\text{I}$ ) 溶液, 移入铂金坩埚中加热至  $1050^\circ\text{C}$  共熔制成熔片, 分析精度优于 5%. 详细实验方法见 Wang *et al.* (2020). 全岩微量元素溶液分析使用 Thermo Scientific iCAP RQ ICP-MS 进行测试, 分析精度一般优于 5%, 详细测试流程参考 Wang *et al.* (2020).

## 3 分析结果

### 3.1 锆石 U-Pb 年代学及原位 Hf 同位素特征

越南中部昆嵩地体 Van Canh 花岗岩体的 4 个样品 (20VN-23, 20VN-24, 20VN-25 和 20VN-29) 的锆石颗粒大多为无色透明的长柱状或短柱状的自形至半自形晶体, 长为  $100 \sim 300 \mu\text{m}$ , 长宽比为  $1:1.5 \sim 1:3$ . 锆石阴极发光图像显示其内部发育有明显的振荡环带 (图 3), 其对应的 Th/U 比值较高, 分别为  $0.60 \sim 1.94$ 、 $0.50 \sim 1.67$ 、 $0.32 \sim 1.61$  和  $0.81 \sim 1.42$ , 反映了岩浆成因锆石的特点 (吴元保和郑永飞, 2004). 锆石 U-Pb 年代学测试结果见附表 1. 二长花岗岩样品 (20VN-23, 20VN-24, 20VN-25) 的锆石加权平均年龄分别为  $239 \pm 2$  Ma (MSWD=0.49,  $N=22$ ; 图 4a)、 $240 \pm 2$  Ma (MSWD=0.16,  $N=17$ ; 图 4b) 和  $244 \pm 2$  Ma (MSWD=0.27,  $N=$

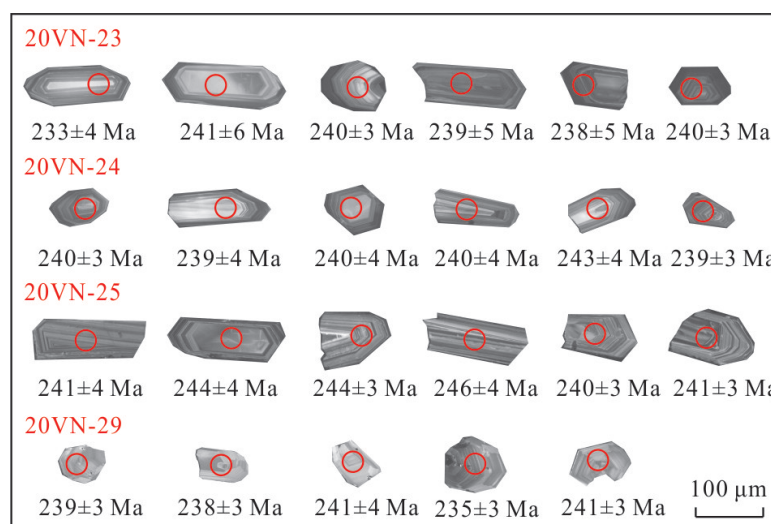


图 3 昆嵩地体南部三叠纪 Van Canh 花岗岩锆石 CL 图像

Fig. 3 Cathodoluminescence (CL) images of the representative zircon grains for the Triassic Van Canh granites in southern Kon-tum massif

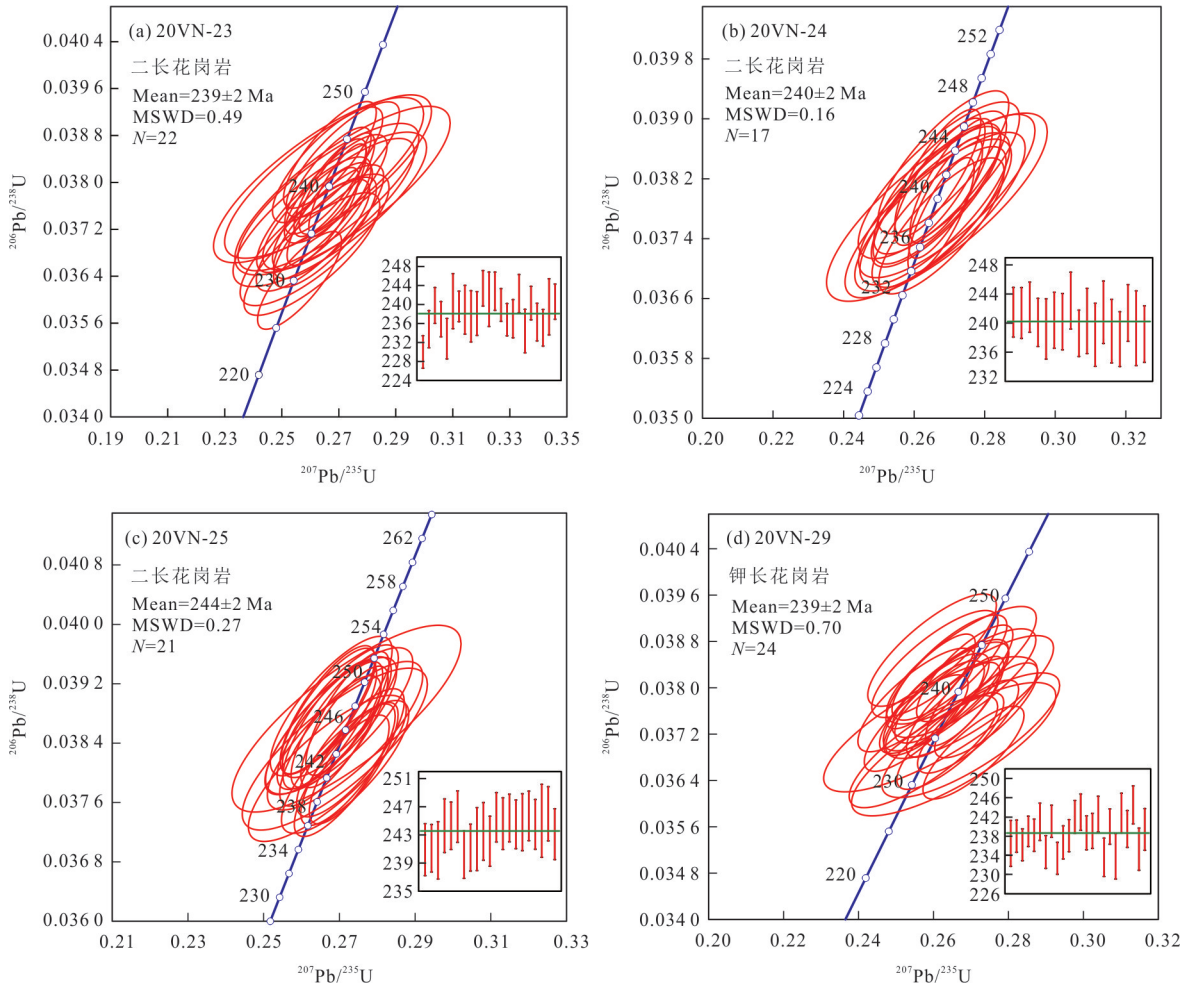


图4 昆嵩地体南部三叠纪 Van Canh 花岗岩锆石 U-Pb 年龄协和图

Fig.4 Zircon U-Pb concordia diagrams for the Triassic Van Canh granites in southern Kontum massif

21; 图 4c), 钾长花岗岩的加权平均年龄为 239±2 Ma (MSWD=0.70, N=24; 图 4d).

作者对 4 件花岗岩的锆石颗粒分别选取了 15 个锆石 U-Pb 测试点进行原位的 Hf 同位素分析, 分析数据结果见附表 2. 其中 3 个二长花岗岩样品具有类似的 Hf 同位素组成, 其锆石  $\epsilon_{\text{Hf}}(t)$  值和二阶段模式年龄 ( $T_{\text{DM2}}$ ) 分别为 -8.5~−0.7 和 1.31~1.81 Ga、−8.5~−1.6 和 1.37~1.80 Ga 以及 −11.2~−3.5 和 1.49~1.98 Ga, 钾长花岗岩 (20VN-29) 的锆石  $\epsilon_{\text{Hf}}(t)$  值和二阶段模式年龄 ( $T_{\text{DM2}}$ ) 分别为 −7.5~−0.8 和 1.32~1.74 Ga. 这些样品的  $\epsilon_{\text{Hf}}(t)$  值与昆嵩地体北部长山带三叠纪 Hai Van 花岗岩 ( $\epsilon_{\text{Hf}}(t)$ =−11.1~−7.7, Hieu *et al.*, 2015) 和昆嵩地体三叠纪花岗岩 ( $\epsilon_{\text{Hf}}(t)$ =−10.6~−6.7; Hung *et al.*, 2022) 相类似(图 5).

### 3.2 岩石地球化学特征

本文三叠纪 Van Canh 花岗岩样品的全岩主量

和微量元素分析结果见附表 3. 样品的烧失量 (LOI) 较低 (0.32%~0.97%), 表明样品未遭受明显的后期蚀变作用. 样品具有较高的  $\text{SiO}_2$  含量 (72.98%~79.37%) 和  $\text{Al}_2\text{O}_3$  含量 (11.41%~13.36%), 较低的  $\text{CaO}$  含量 (0.08%~0.87%)、 $\text{Fe}_2\text{O}_3$  含量 (0.25%~4.00%)、 $\text{MgO}$  含量 (0.03%~0.54%)、 $\text{TiO}_2$  含量 (0.08%~0.24%) 和  $\text{P}_2\text{O}_5$  含量 (0.01%~0.06%). CIPW 标准化矿物计算显示其体积含量为: 石英 (33.6%~44.0%)、正长石 (27.6%~34.4%)、钠长石 (17.8%~28.2%)、钙长石 (0.36%~4.17%) 和刚玉分子 (0.49%~2.30%). 所有样品在 An-Ab-Or 三角图解主要落在了花岗岩区域(图 6a). 样品具有较高的全碱 ( $\text{K}_2\text{O} + \text{Na}_2\text{O}$ =6.97%~8.80%) 含量和较高的  $\text{K}_2\text{O}/\text{Na}_2\text{O}$  (1.40~2.32) 比值, 在  $\text{K}_2\text{O}-\text{SiO}_2$  图解中(图 6b), 样品落于高钾钙碱性系列. 样品的铝饱和指数 A/CNK 值介于 1.03~1.21, 其 A/NK 值介于 1.13~1.40, 具有过铝质花岗岩的特征(图 6c). 在

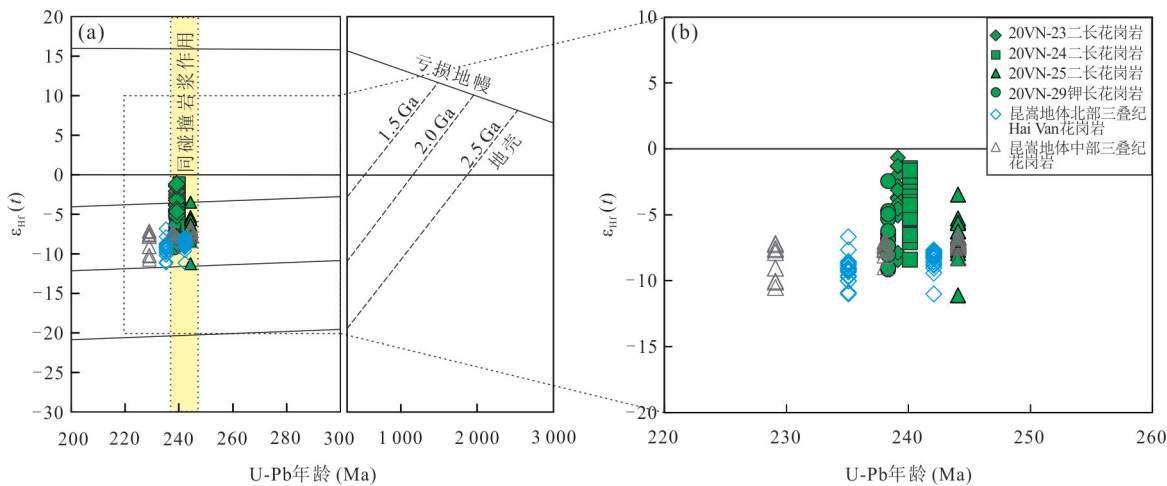
图 5 昆嵩地体南部三叠纪 Van Canh 花岗岩锆石  $\epsilon_{\text{Hf}}(t)$ —年龄(Ma)图解

Fig. 5 Plot of  $\epsilon_{\text{Hf}}(t)$  vs. age (Ma) for zircon grains from the Triassic Van Canh granites in southern Kontum massif  
背景数据引自 Hieu et al. (2015); Wang et al. (2018); Hung et al. (2022)

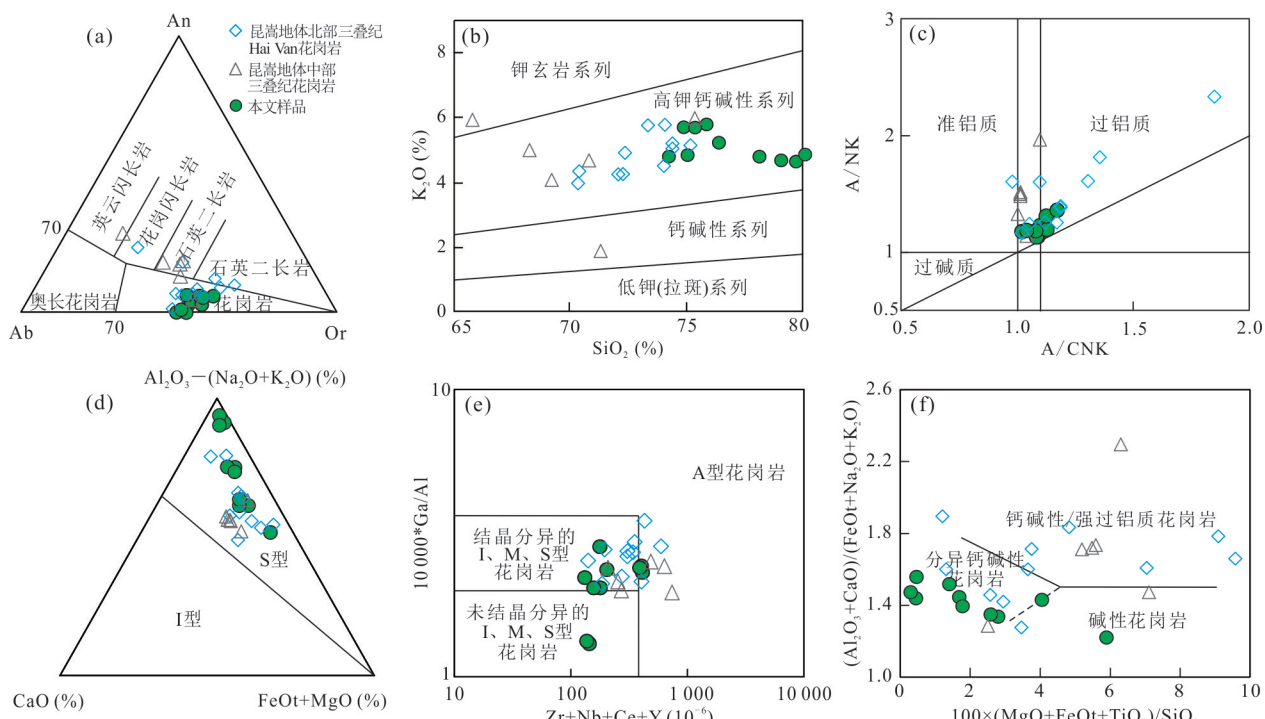


图 6 昆嵩地体南部三叠纪 Van Canh 花岗岩

Fig. 6 Triassic Van Canh granites in southern Kontum massif

a. An—Ab—Or 判别图解; b.  $K_2O$ — $SiO_2$  判别图解; c.  $A/NK$ — $A/CNK$  判别图解; d.  $(Al_2O_3-(Na_2O+K_2O))$ — $CaO$ — $(FeOt+MgO)$  判别图解; e.  $10000*Ga/Al$ — $(Zr+Nb+Ce+Y) \times 10^{-6}$  判别图解; f.  $(Al_2O_3+CaO)/(FeOt+Na_2O+K_2O)$ — $100 \times (MgO+FeOt+TiO_2)/SiO_2$  判别图解。  
图 a~f 背景数据引自 Hieu et al. (2015) 和 Hung et al. (2022); 图 b 据 Winchester and Floyd (1977); 图 d 据 Chappell and White (1992); 图 e 据 Whalen et al. (1987); 图 f 据 Sylvester (1989)

哈克图解中,除  $K_2O$  和  $Na_2O$  趋势不明显外,  $Al_2O_3$ 、 $Fe_2O_3$ 、 $MgO$ 、 $CaO$ 、 $TiO_2$  和  $P_2O_5$  与  $SiO_2$  均呈负相关关系。样品主量元素特征总体也与昆嵩地体北部的长山带三叠纪 Hai Van 花岗岩以及昆嵩地体中部三叠纪花岗质岩石相类似(Hieu et al., 2015; Hung

et al., 2022) (图 7)。

本文三叠纪 Van Canh 花岗岩样品的稀土元素总量 ( $\sum REE$ ) 较高,为  $38.2 \times 10^{-6} \sim 254.2 \times 10^{-6}$  g/g, 球粒陨石标准化稀土元素配分图解具有显著的右倾特征,轻重稀土分异明显(图 8a),其  $(La/Yb)_N$

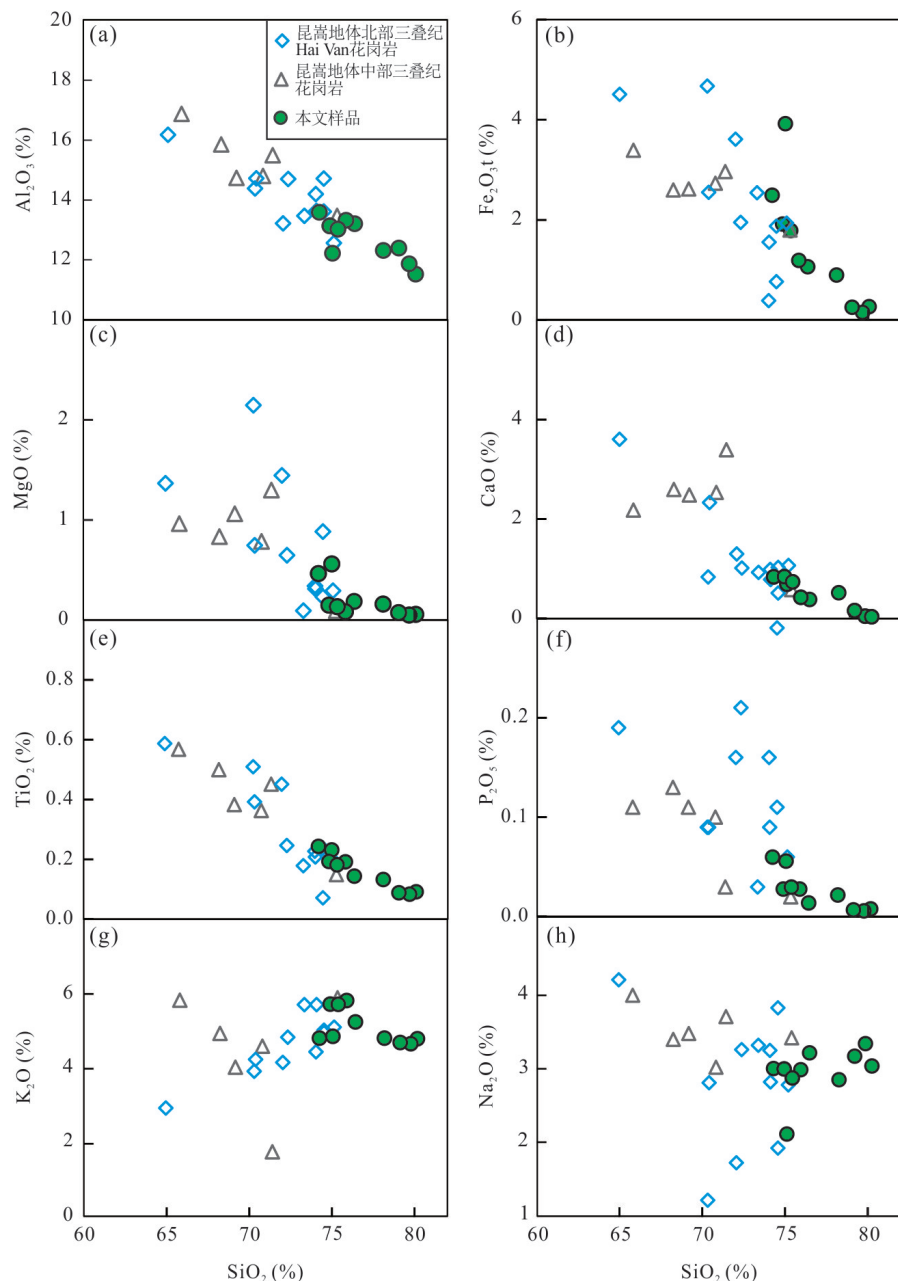


图7 昆嵩地体南部三叠纪 Van Canh 花岗岩哈克图解

Fig. 7 Harker diagrams for the Triassic Van Canh granites in southern Kontum massif  
背景数据引自 Hieu *et al.* (2015); Hung *et al.* (2022)

为 $1.85\sim16.27$ ,  $(\text{Gd}/\text{Yb})_{\text{N}}$ 为 $0.73\sim2.19$ , 并具明显的Eu负异常( $\text{Eu}/\text{Eu}^* = 0.24\sim0.56$ )。在原始地幔标准化微量元素蛛网图中(图8b), 样品显示出大离子亲石元素的富集( $\text{Rb}$ 、 $\text{Th}$ 、 $\text{U}$ )和高场强元素的亏损( $\text{Nb}$ 、 $\text{Ta}$ 、 $\text{Ti}$ ), 并具有明显的Sr和Ba的负异常。此外, 本文样品显示出与长山带三叠纪Hai Van花岗岩相类似的稀土和微量元素配分模式特征(图8; Hieu *et al.*, 2015)。

## 4 讨论

### 4.1 岩石成因

本文花岗岩样品在微量元素上具有明显的Ba和Sr负异常, 结合Rb-Sr和Ba-Sr图解(图9b~9c)的特征, 表明该套花岗岩样品在演化过程中发生了明显的斜长石和钾长石的分离结晶。此外, 样品显示强烈的P亏损(图8), 表明其可能经历了磷灰石的分离结晶。部分样品具有高的硅含量( $>75\%$ ),

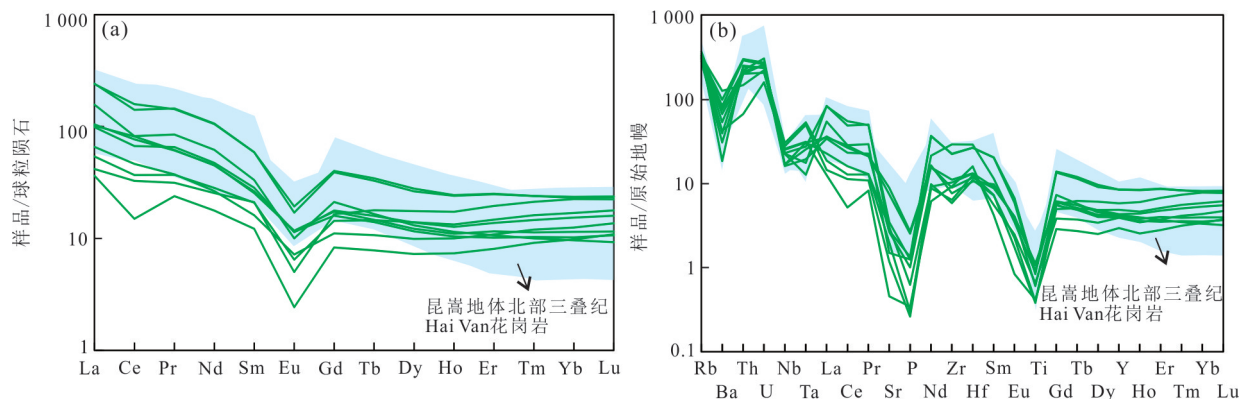


图 8 昆嵩地体南部三叠纪 Van Canh 花岗岩球粒陨石标准化稀土元素配分曲线(a)和原始地幔标准化微量元素蛛网图(b)  
Fig. 8 Chondrite-normalized REE patterns (a) and primitive mantle-normalized trace element spidergram (b) for the Triassic Van Canh granites in southern Kontum massif

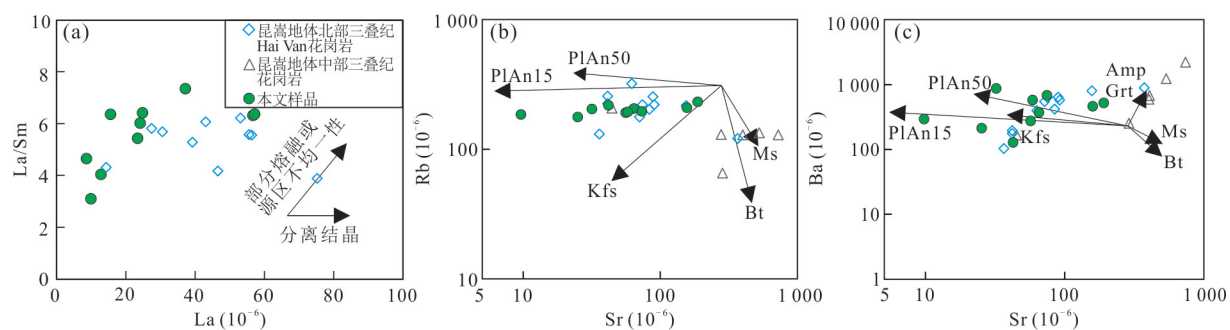


图 9 昆嵩地体南部三叠纪 Van Canh 花岗岩 La/Sm-La (a)、Rb-Sr (b) 和 Ba-Sr (c) 图解  
Fig. 9 Plots of La/Sm vs. La (a), Rb vs. Sr (b) and Ba vs. Sr (c) for the Triassic Van Canh granites in southern Kontum massif  
背景数据引自 Hieu *et al.* (2015); Hung *et al.* (2022); 图 b 和图 c 据 Li *et al.* (2007)

且镜下可见少量锂云母矿物(图 2e),暗示其高演化的特征(吴福元等, 2017).花岗岩的分异指数 DI (DI=Q+Or+Ab+Ne+Lc+Kp)较高,为89~98,结合其强烈的Eu负异常及“海鸥状”的稀土元素配分模式,均显示出与高分异花岗岩相似的地球化学特征(图 8a; Wu *et al.*, 2017).在图 6f 中,样品也主要落在了分异型的钙碱性花岗岩区域内,同时样品的锆石Zr/Hf比值为0.16~16.68(<25),进一步证实了其高分异的特征(Breiter *et al.*, 2014).此外,花岗岩的稀土元素四分组强度TE<sub>1,3</sub>为0.85~1.02(<1.1),表明岩浆演化中不存在明显的流体—熔体相互作用.因此,本文花岗岩样品应为无流体相的高分异花岗岩(如陶继华等, 2013; Ballouard *et al.*, 2016; 余小清等, 2021).样品的10 000×Ga/Al值为1.30~2.83,Zr+Nb+Ce+Y平均含量为234×10<sup>-6</sup>,均低于Whalen *et al.* (1987)提出的A型花岗岩元素含量,而落入结晶分异的I、M、S型花岗岩区域.此外,样品镜下无明显的碱性暗色矿物,并可见

S型花岗岩常见的白云母等特征矿物,其铝饱和指数较高(1.03~1.21),CIPW标准矿物中的刚玉体积含量均大于1%.上述这些特征结合图解 6d,均表明本文的样品属于高分异 S型花岗岩.

本文花岗岩具有较低的CaO值(0.08%~0.87%)和变化较大的Al<sub>2</sub>O<sub>3</sub>/(FeOt+MgO)值(2.92~74.7),表明该花岗岩样品可能主要源自变沉积岩源区,混有少量变火成岩(图 10a, Laurent *et al.*, 2014).在图 10b 中,本文样品主要落在泥质岩部分熔融区域,个别落在角闪岩部分熔融区域内.一般的单一岩浆源区的火成岩具有比较均一的La/Ce 和 Rb/Ti 比值(Marjorie, 1993),而本文花岗岩具有变化的La/Ce 比值(0.48~0.94)和Rb/Ti 比值(0.15~0.43),暗示它们存在混合源区的特征.本文样品在野外于岩体中部采样,且岩体内未发现有围岩同化混染相关的捕虏体(李名则等, 2020),也未见围岩同化混染导致的结构构造不均一的现象.此外, Yang *et al.* (2007)认为围岩同化混染过程会导

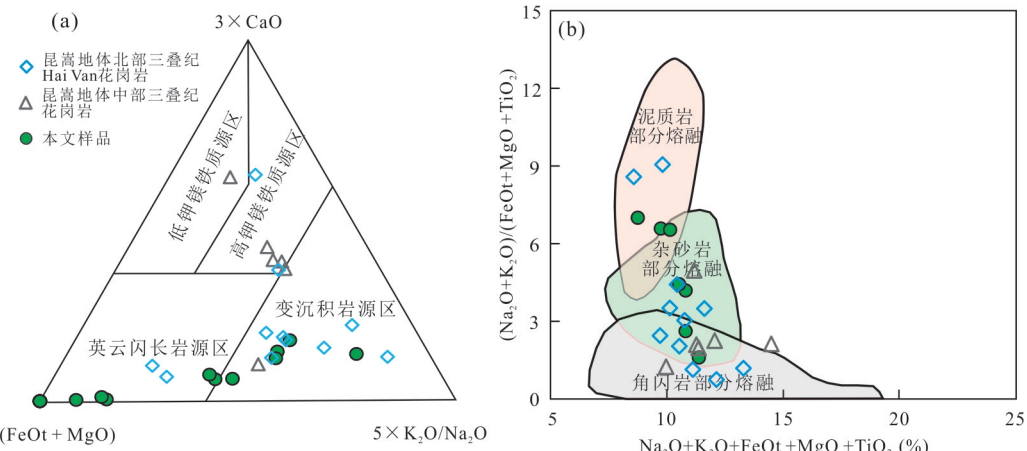


图10 昆嵩地体南部三叠纪 Van Canh 花岗岩  $3 \times \text{CaO}$ — $\text{Al}_2\text{O}_3/(\text{FeOt} + \text{MgO})$ — $5 \times \text{K}_2\text{O}/\text{Na}_2\text{O}$ (a) 和  $(\text{Na}_2\text{O} + \text{K}_2\text{O})/(\text{FeOt} + \text{MgO} + \text{TiO}_2)$ — $(\text{Na}_2\text{O} + \text{K}_2\text{O} + \text{FeOt} + \text{MgO} + \text{TiO}_2)$ (b) 图解

Fig. 10 Plots of  $3 \times \text{CaO}$  vs.  $\text{Al}_2\text{O}_3/(\text{FeOt} + \text{MgO})$  vs.  $5 \times \text{K}_2\text{O}/\text{Na}_2\text{O}$  (a) and  $(\text{Na}_2\text{O} + \text{K}_2\text{O})/(\text{FeOt} + \text{MgO} + \text{TiO}_2)$  vs.  $\text{Na}_2\text{O} + \text{K}_2\text{O} + \text{FeOt} + \text{MgO} + \text{TiO}_2$  (b) for the Triassic Van Canh granites in southern Kontum massif

对比数据引自 Hieu *et al.* (2015); Hung *et al.* (2022); 背景数据 Laurent *et al.* (2014); Patino Douce and Harris (1998); Patino Douce (1999)

致侵入体中含有从围岩中捕获的继承锆石,而本文样品锆石均为岩浆成因锆石,年龄均一,未见继承锆石。因此,本文样品应该未受明显的围岩同化混染作用。样品的锆石具有富集且变化范围较大的 $\epsilon_{\text{Hf}}(t)$ 值( $-11.2 \sim -0.7$ ),这个特征结合 La/Sm—La 图解均表明本文样品具有源区不均一性的特征(图 9a)。此外,样品富集的 Hf 同位素及较老的 Hf 二阶模式年龄( $T_{\text{DM2}}=1.31 \sim 1.98$  Ga),均与区域上马江带 Muong Lat 花岗岩( $251 \sim 235$  Ma,  $\epsilon_{\text{Hf}}(t) = -13.1 \sim -9.4$ ,  $T_{\text{DM2}}=1.87 \sim 2.07$  Ga, 如 van Thanh *et al.*, 2019)和 Phia Bioc 花岗岩( $244$  Ma,  $\epsilon_{\text{Hf}}(t) = -10.0 \sim -6.6$ ,  $T_{\text{DM2}}=1.17 \sim 1.35$  Ga, Hieu *et al.*, 2017)、长山带 Hai Van 花岗岩( $242 \sim 224$  Ma,  $\epsilon_{\text{Hf}}(t) = -11.1 \sim -7.7$ ,  $T_{\text{DM2}}=1.69 \sim 1.98$  Ga, Hieu *et al.*, 2015)以及昆嵩地体中部花岗岩( $251 \sim 229$  Ma,  $\epsilon_{\text{Hf}}(t) = -11.1 \sim -6.7$ ,  $T_{\text{DM2}}=1.70 \sim 1.97$  Ga, Hung *et al.*, 2022)等主要来源于“古老”地壳部分熔融的花岗岩相一致。综合昆嵩地体古生代—中生代沉积岩碎屑锆石的主要峰值特征( $1.44$  Ga 和  $1.78 \sim 1.80$  Ga)(Kawaguchi *et al.*, 2021),作者认为本文花岗岩源自古—中元古代变泥质岩部分熔融,并有少量变火成岩的加入。

#### 4.2 区域对比与构造意义

印支运动传统被认为是与古特提斯洋的俯冲—闭合有关,并导致了印支陆块广泛发育二叠纪—三叠纪的构造热事件及相关岩浆—变质作用

(Carter *et al.*, 2001; Lepvrier *et al.*, 2004, 2008; Metcalfe, 2013; Faure *et al.*, 2014). 随着马江古特提斯分支洋的俯冲闭合及随后的印支与华南陆块碰撞拼贴,在印支陆块东北部形成了长山构造岩浆岩带,而该带也是东南亚最重要的多金属成矿带(Kamvong *et al.*, 2014; Tran *et al.*, 2014; Manaka *et al.*, 2014). 也有学者认为,该区大规模侵位的三叠纪花岗岩为区域成矿提供了大量的热量和成矿物质,如深部的岩浆热液通过断层运移与较浅地壳中的大气水混合形成了越南北部的 Binh Do 铅锌矿床(Huang *et al.*, 2019). 已有的研究在长山带老挝境内及越南北部识别出了大量晚古生代  $306 \sim 260$  Ma 与马江支洋盆俯冲有关的岛弧岩浆作用(图 1a; Liu *et al.*, 2012; Tran *et al.*, 2014; Shi *et al.*, 2015; Hieu *et al.*, 2016, 2017, 2020; Pham *et al.*, 2018; Qian *et al.*, 2019). 此外,在该带及其周缘地区还识别出了大量的晚二叠世晚期—三叠纪的岩浆及变质事件的记录,如越南北部马江带的 Muong Lat 花岗岩( $251 \sim 235$  Ma, van Thanh *et al.*, 2019);老挝北部的 Lat Boua 花岗岩( $255 \sim 245$  Ma)、Kham 花岗岩( $253 \sim 234$  Ma)、Phon Thong 花岗岩( $250 \sim 245$  Ma)、Lua 花岗岩( $239 \sim 234$  Ma)和 Na The 花岗岩( $256 \sim 240$  Ma)(Wang *et al.*, 2016c);越南西北部奠边地区花岗岩( $242 \sim 225$  Ma, Roger *et al.*, 2014; Shi *et al.*, 2015; Hieu *et al.*, 2020)以及越南中部的 Hai Van 花岗岩( $242 \sim 224$  Ma, Hieu *et al.*,

2015)等。变质作用的研究也表明长山带及周缘的变质作用主要发生在早三叠世之后,如越北 Nam Co 组和马江组糜棱岩的变形年龄为~250~240 Ma (Maluska *et al.*, 2005; Liu *et al.*, 2012; 钱鑫等, 2022)。此外,马江带榴辉岩的锆石和独居石 U-Pb 年龄分别为  $230 \pm 8$  Ma 和  $243 \pm 4$  Ma, 类似同期泥质麻粒岩的进变质时代和同造山期的构造热时代, 分别为  $233 \pm 5$  Ma 和 ~ $251 \sim 229$  Ma (Lepvrier *et al.*, 1997, 2004; Nakano *et al.*, 2008, 2010; Zhang *et al.*, 2013, 2014)。在越南中部昆嵩地体同样也记录了显著的三叠纪时期的变质热事件, 其年龄多集中在  $251 \sim 222$  Ma (图 12, 如 Tran, 1998; Carter *et al.*, 2001; Lan *et al.*, 2003; Maluska *et al.*, 2005; Owada *et al.*, 2006, 2007, 2016; Nakano *et al.*, 2013)。近年来,也有部分学者在昆嵩地体中部的中生代岩体中识别出了三叠纪( $251 \sim 229$  Ma)时期的花岗质岩石(Tinh *et al.*, 2021; Cuong *et al.*, 2021; Hung *et al.*, 2022)。而本文研究的花岗岩样品位于昆嵩地体南部的 Van Canh 花岗岩, 其形成时代为中三叠世( $244 \sim 239$  Ma), 与昆嵩地体和长山带同期岩浆和变质事件相一致(图 12), 表明该区这一系列三叠纪火成岩可从老越交界的马江地区经长山带向南延伸至越南中部昆嵩地区, 证实了整个越南中部地区均经历了强烈的晚二叠世—三叠纪的印支造山运动。

Wang *et al.* (2018) 系统综述了长山带和金沙江—哀牢山—马江古特提斯带内的火成岩, 并综合提出 3 阶段的构造演化过程: 初始闭合 (~247 Ma)、同碰撞 (~247~237 Ma) 和碰撞后 (~237~200 Ma) 的演化模型。已有的研究也表明越南西北部马江带中的 I 型和 S 型花岗岩均与晚二叠世—早三叠世期间印支与华南地块的碰撞拼合有关(Hieu *et al.*, 2017, 2020; van Thanh *et al.*, 2019)。随后, 在中一晚三叠世(~237~220 Ma), 由于碰撞后重力崩塌和区域热梯度的变化, 引起了软流圈上涌造成了中一下地壳物质发生大规模的部分熔融, 从而形成了长山带晚三叠世花岗质岩浆 (Qian *et al.*, 2019; 钱鑫等, 2022)。但是, 对于昆嵩地体二叠纪—三叠纪长英质火成岩的成因则存在不同观点, 包括了峨眉山地幔柱成因和碰撞造山成因。部分学者认为地幔柱可引发大规模岩浆侵入到昆嵩地体深部, 并作为热源诱发了下地壳的部分熔融和超高温变质作用, 从而形成区域变质岩及相对

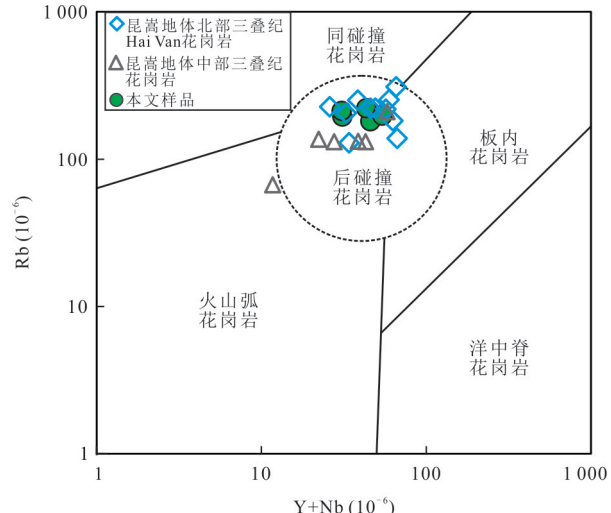


图 11 昆嵩地体南部三叠纪 Van Canh 花岗岩构造环境判别图

Fig. 11 Tectonic discrimination diagram for the Triassic Van Canh granites in southern Kontum massif

背景数据引自 Hieu *et al.* (2015); Hung *et al.* (2022); 图据 Pearce *et al.* (1996)

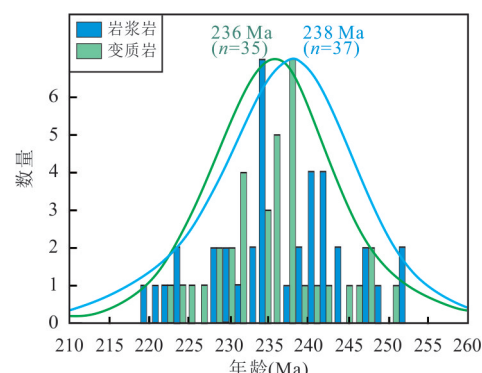


图 12 昆嵩地体三叠纪已发表岩浆岩和变质岩年龄汇总  
(年龄数据见附表 4)

Fig 12 Summary of the published Triassic ages for the igneous and metamorphic rocks from the Kontum massif

应的花岗质岩石(Owada *et al.*, 2007, 2016, 2020; Osanai *et al.*, 2008)。而大部分学者则认为该期岩浆活动与印支和华南陆块的碰撞造山有关(Hoa *et al.*, 2008; Nakano *et al.*, 2013, 2021; Hieu *et al.*, 2015, 2017, 2020; van Thanh *et al.*, 2019)。目前,已有研究显示峨眉山大火成岩省仅局限于中国西南部和越南东北部松大裂谷地区, 尚无明显证据显示其分布在马江缝合带西南部(Liu *et al.*, 2012; Hieu *et al.*, 2016; Qian *et al.*, 2019)。因此, 结合上述区域大规模的岩浆及变质作用, 作者认为越

南中部昆嵩地体这套 Van Canh 花岗岩的形成与马江古特提斯分支洋闭合后的印支和华南陆块的碰撞拼贴有关。

如前所述,昆嵩地体广泛发育三叠纪高温或伸展相关的岩浆及变质记录以及相对应的构造变形。越南中部 Song Ba 河地区的 Kannack 紫苏花岗岩的岩浆形成与侵位时间一致,具有相似的锆石 U-Pb 年龄(249 Ma)和黑云母 Ar-Ar 年龄(243 Ma),表明早三叠世期间的新生地壳快速剥露,暗示该区可能已经进入大陆碰撞期间(Nagy *et al.*, 2001)。昆嵩地体中部~247 Ma 的 Ngoc Linh 榴辉岩和~248 Ma 的 Kannak 超高压麻粒岩相变质岩具有减压的 P-T 轨迹,表明其具有伸展的构造背景(Osanai *et al.*, 2004; Nakano *et al.*, 2007, 2013; Zheng *et al.*, 2021)。此外,保存在昆嵩地体的同变质构造事件主要发育于早三叠世的伸展构造环境中,并造成地壳发生广泛的部分熔融,形成了普遍发育北西—南东向拉伸线理的 Ngoc Linh 变质核杂岩,随后在 240~224 Ma Ngoc Linh 变质核杂岩叠加了右旋走滑断层(Faure *et al.*, 2018)。因此,这些岩浆、变质和变形的地质记录均显示昆嵩地体在~240 Ma 已进入后碰撞阶段。一般来说,高钾钙碱性火成岩主要形成于造山期由挤压向伸展转换的环境中(邓晋福等, 2004)。而已有的研究表明长山带和马江带广泛发育三叠纪高钾钙碱性花岗岩,包括形成于后碰撞构造背景的奠边府花岗岩、Muong Luan I型花岗岩、老挝北部花岗岩和昆嵩地体北部的 Hai Van 花岗岩(Liu *et al.*, 2012; Hieu *et al.*, 2015, 2020; Qian *et al.*, 2019; van Thanh *et al.*, 2019)。昆嵩地体中部 Van Canh 花岗岩也显示高钾钙碱性的特征(Hieu *et al.*, 2015; Hung *et al.*, 2022)。因此,本文研究的中三叠世 Van Canh 高钾钙碱性花岗岩及区域同期花岗岩均具有类似的后碰撞地球化学特征,且在构造判别图上也都落在后碰撞的构造背景(图 11),表明越南中部昆嵩地区广泛发育中—晚三叠世后碰撞相关的岩浆作用。前人研究表明,在后碰撞伸展背景下,由于加厚的岩石圈拆沉和软流圈底侵,岩石圈上部部分熔融可以形成花岗质岩石(Huang *et al.*, 2019; 徐畅等, 2020)。综合上述分析,认为本文昆嵩地区的中三叠世花岗质岩石均形成于后碰撞的伸展背景。由于马江古特提斯分支洋的俯冲闭合导致了印支和华南陆块在晚二叠世—早三叠世发生碰撞拼合,并在随后的中三叠世进入到后碰撞

阶段,加厚地壳发生拆沉,软流圈物质上涌导致了区域的伸展作用,并造成了“古老的”变沉积岩和变火山岩发生大规模部分熔融,从而形成了昆嵩地体内部广泛分布的中—晚三叠世高钾钙碱性花岗质岩石。

## 5 结论

(1) 昆嵩地体南部 Van Canh 花岗岩的锆石 U-Pb 年龄为 244~239 Ma, 为中三叠世, 其锆石原位  $\epsilon_{\text{Hf}}(t)$  值为 -11.2~-0.7。

(2) 昆嵩地体南部 Van Canh 花岗岩为高钾钙碱性的高分异 S 型花岗岩,源自古—中元古代变泥质岩部分熔融,并有少量变火成岩的加入。

(3) Van Canh 中三叠世花岗岩形成于后碰撞背景,与印支和华南陆块的碰撞拼合后的地壳拆沉有关。

致谢:野外工作及实验分析得到了中山大学王玉琨博士、甘成势博士以及杨雪博士的帮助,审稿专家和编辑部老师对本文提出了宝贵的修改意见,在此一并致以衷心的感谢。

附表见本刊官网(<http://www.earth-science.net>)。

## References

- Acharyya, S. K., 1998. Break-up of the Greater Indo-Australian Continent and Accretion of Blocks Framing South and East Asia. *Journal of Geodynamics*, 26(1): 149—170. [https://doi.org/10.1016/S0264-3707\(98\)00012-X](https://doi.org/10.1016/S0264-3707(98)00012-X)
- Ballouard, C., Poujol, M., Boulvais, P., et al., 2016. Nb-Ta Fractionation in Peraluminous Granites: A Marker of the Magmatic-Hydrothermal Transition. *Geology*, 44 (3): 231—234. <https://doi.org/10.1130/g37475.1>
- Blichert-Toft, J., Albarède, F., 1997. The Lu-Hf Isotope Geochemistry of Chondrites and the Evolution of the Mantle-Crust System. *Earth and Planetary Science Letters*, 148(1—2): 243—258. [https://doi.org/10.1016/s0012-821x\(97\)00040-x](https://doi.org/10.1016/s0012-821x(97)00040-x)
- Breiter, K., Lamarão, C. N., Borges, R. M. K., et al., 2014. Chemical Characteristics of Zircon from A-Type Granites and Comparison to Zircon of S-Type Granites. *Lithos*, 192/193/194/195: 208—225. <https://doi.org/10.1016/j.lithos.2014.02.004>
- Bullard, E. C., Everett, J. E., Smith, A. G., 1965. The Fit of the Continents around the Atlantic: Asymposium on Continental Drift. *Philosophical Transactions of the Roy-*

- al Society, London, Serial A, 258(1088): 41—51.
- Carter, A., Roques, D., Bristow, C., et al., 2001. Understanding Mesozoic Accretion in Southeast Asia: Significance of Triassic Thermotectonism (Indosinian Orogeny) in Vietnam. *Geology*, 29(3): 211. [https://doi.org/10.1130/0091-7613\(2001\)0290211:umaisa>2.0.co;2](https://doi.org/10.1130/0091-7613(2001)0290211:umaisa>2.0.co;2)
- Chappell, B. W., White, A. J. R., 1992. I- and S-Type Granites in the Lachlan Fold Belt. *Earth and Environmental Science Transactions of the Royal Society of Edinburgh*, 83(1/2): 1—26. <https://doi.org/10.1017/s0263593300007720>
- Chung, S. L., Lee, T. Y., Lo, C. H., et al., 1997. Intraplate Extension Prior to Continental Extrusion along the Ailao Shan-Red River Shear Zone. *Geology*, 25(4): 311—314. [https://doi.org/10.1130/0091-7613\(1997\)0250311:iaptce>2.3.co;2](https://doi.org/10.1130/0091-7613(1997)0250311:iaptce>2.3.co;2)
- Cuong, T. C., Hieu, P. T., Minh, P., et al., 2021. Zircon U-Pb Ages of the Pegmatites in the Kontum Massif, Central Vietnam and Their Quality Evaluation for Ceramic Industry. *Journal of Mineralogical and Petrological Sciences*, 116(6): 279—292. <https://doi.org/10.2465/jmps.210911>
- Deng, J. F., Luo, Z. H., Su, S. G., et al., 2004. Petrogenesis, Tectonic Environment and Mineralization. *Geology Press*, Beijing (in Chinese).
- Faure, M., Lepvrier, C., Van Nguyen, V., et al., 2014. The South China Block-Indochina Collision: Where, When, and How? *Journal of Asian Earth Sciences*, 79: 260—274. <https://doi.org/10.1016/j.jseas.2013.09.022>
- Faure, M., Nguyen, V. V., Hoai, L. T. T., 2018. Early Paleozoic or Early-Middle Triassic Collision between the South China and Indochina Blocks: The Controversy Resolved? Structural Insights from the Kon Tum Massif (Central Vietnam). *Journal of Asian Earth Sciences*, 166: 162—180. <https://doi.org/10.1016/j.jseas.2018.07.015>
- Griffin, W.L., Wang, X., Jackson, S.E., et al., 2002. Zircon Chemistry and Magma Mixing, SE China: In-Situ Analysis of Hf Isotopes, Tonglu and Pingtan Igneous Complexes. *Lithos*, 61(3/4): 237—269. [https://doi.org/10.1016/S0024-4937\(02\)00082-8](https://doi.org/10.1016/S0024-4937(02)00082-8)
- Griffin, W. L., Powell, W. J., Pearson, N. J., et al., 2008. GLITTER: Data Reduction Software for Laser Ablation ICP-MS Laser Ablation-ICP-MS in the Earth Sciences. *Mineralogical Association of Canada, Short Course Series*, 40: 204—207.
- Hieu, P. T., Anh, N. T. Q., Minh, P., et al., 2020. Geochemistry, Zircon U-Pb Ages and Hf Isotopes of the Muong Luan Granitoid Pluton, Northwest Vietnam and Its Petrogenetic Significance. *Island Arc*, 29(1): e12330. <https://doi.org/10.1111/iar.12330>
- Hieu, P. T., Chen, F. K., Me, L. T., et al., 2012. Zircon U-Pb Ages and Hf Isotopic Compositions from the Sin Quyen Formation: The Precambrian Crustal Evolution of Northwest Vietnam. *International Geology Review*, 54(13): 1548—1561. <https://doi.org/10.1080/00206814.2011.646831>
- Hieu, P. T., Chen, F. K., Thuy, N. T. B., et al., 2013. Geochemistry and Zircon U-Pb Ages and Hf Isotopic Composition of Permian Alkali Granitoids of the Phan Si Pan Zone in Northwestern Vietnam. *Journal of Geodynamics*, 69: 106—121. <https://doi.org/10.1016/j.jog.2012.03.002>
- Hieu, P. T., Dung, N. T., Thuy, N. T. B., et al., 2016. U-Pb Ages and Hf Isotopic Composition of Zircon and Bulk Rock Geochemistry of the Dai Loc Granitoid Complex in Kontum Massif: Implications for Early Paleozoic Crustal Evolution in Central Vietnam. *Journal of Mineralogical and Petrological Sciences*, 111(5): 326—336. <https://doi.org/10.2465/jmps.151229>
- Hieu, P. T., Li, S. Q., Yu, Y., et al., 2017. Stages of Late Paleozoic to Early Mesozoic Magmatism in the Song Ma Belt, NW Vietnam: Evidence from Zircon U-Pb Geochronology and Hf Isotope Composition. *International Journal of Earth Sciences*, 106(3): 855—874. <https://doi.org/10.1007/s00531-016-1337-9>
- Hieu, P. T., Yang, Y. Z., Binh, D. Q., et al., 2015. Late Permian to Early Triassic Crustal Evolution of the Kontum Massif, Central Vietnam: Zircon U-Pb Ages and Geochemical and Nd-Hf Isotopic Composition of the Hai van Granitoid Complex. *International Geology Review*, 57(15): 1877—1888. <https://doi.org/10.1080/00206814.2015.1031194>
- Hoa, T. T., Polyakov, G. V., Tran, T. A., et al., 2016. Intraplate Magmatism and Metallogeny of North Vietnam. In: Dilek, Y., Pirajno, F., Windley, B., eds., *Modern Approaches in Solid Earth Sciences*. Springer International Publishing, Switzerland, 372.
- Hoa, T. T., Anh, T. T., Phuong, N. T., et al., 2008. Permo-Triassic Intermediate-Felsic Magmatism of the Truong Son Belt, Eastern Margin of Indochina. *Comptes Rendus Geoscience*, 340(2/3): 112—126. <https://doi.org/10.1016/j.crte.2007.12.002>
- Hu, Z. C., Liu, Y. S., Gao, S., et al., 2012. Improved In Situ Hf Isotope Ratio Analysis of Zircon Using Newly Designed X Skimmer Cone and Jet Sample Cone in

- Combination with the Addition of Nitrogen by Laser Ablation Multiple Collector ICP-MS. *Journal of Analytical Atomic Spectrometry*, 27(9): 1391. <https://doi.org/10.1039/c2ja30078h>
- Huang, C. W., Li, H., Lai, C. K., 2019. Genesis of the Binh do Pb-Zn Deposit in Northern Vietnam: Evidence from H-O-S-Pb Isotope Geochemistry. *Journal of Earth Science*, 30(4): 679–688. <https://doi.org/10.1007/s12583-019-0872-2>
- Hung, D. D., Tsutsumi, Y., Hieu, P. T., et al., 2022. Van Canh Triassic Granite in the Kontum Massif, Central Vietnam: Geochemistry, Geochronology, and Tectonic Implications. *Journal of Asian Earth Sciences*: X, 7: 100075. <https://doi.org/10.1016/j.jaesx.2021.100075>
- Hutchison, C. S., 1989. The Palaeo-Tethyan Realm and Indosinian Orogenic System of Southeast Asia. Tectonic Evolution of the Tethyan Region. Springer, Dordrecht, 585–643. [https://doi.org/10.1007/978-94-009-2253-2\\_25](https://doi.org/10.1007/978-94-009-2253-2_25)
- Jian, P., Liu, D. Y., Kröner, A., et al., 2009. Devonian to Permian Plate Tectonic Cycle of the Paleo-Tethys Orogen in Southwest China (II): Insights from Zircon Ages of Ophiolites, Arc/back-Arc Assemblages and Within-Plate Igneous Rocks and Generation of the Emeishan CFB Province. *Lithos*, 113(3/4): 767–784. <https://doi.org/10.1016/j.lithos.2009.04.006>
- Jiang, W., Yu, J. H., Wang, X., et al., 2020. Early Paleozoic Magmatism in Northern Kontum Massif, Central Vietnam: Insights into Tectonic Evolution of the Eastern Indochina Block. *Lithos*, 376/377: 105750. <https://doi.org/10.1016/j.lithos.2020.105750>
- Jung, S., Albert Pfänder, J., 2007. Source Composition and Melting Temperatures of Orogenic Granitoids: Constraints from CaO/Na<sub>2</sub>O, Al<sub>2</sub>O<sub>3</sub>/TiO<sub>2</sub> and Accessory Mineral Saturation Thermometry. *European Journal of Mineralogy*, 19(6): 859–870. <https://doi.org/10.1127/0935-1221/2007/0019-1774>
- Kamvong, T., Zaw, K., Meffre, S., et al., 2014. Adakites in the Truong Son and Loei Fold Belts, Thailand and Laos: Genesis and Implications for Geodynamics and Metallogeny. *Gondwana Research*, 26(1): 165–184. <https://doi.org/10.1016/j.gr.2013.06.011>
- Kawaguchi, K., Minh, P., Hieu, P. T., et al., 2021. Evolution of Supracrustal Rocks of the Indochina Block: Evidence from New Detrital Zircon U-Pb Ages of the Kontum Massif, Central Vietnam. *Journal of Mineralogical and Petrological Sciences*, 116(2): 69–82. <https://doi.org/10.2465/jmps.200916>
- Lan, C. Y., Chung, S. L., Van Long, T., et al., 2003. Geochemical and Sr-Nd Isotopic Constraints from the Kontum Massif, Central Vietnam on the Crustal Evolution of the Indochina Block. *Precambrian Research*, 122(1–4): 7–27. [https://doi.org/10.1016/s0301-9268\(02\)00205-x](https://doi.org/10.1016/s0301-9268(02)00205-x)
- Laurent, O., Martin, H., Moyen, J. F., et al., 2014. The Diversity and Evolution of Late-Archean Granitoids: Evidence for the Onset of “Modern-Style” Plate Tectonics between 3.0 and 2.5 Ga. *Lithos*, 205: 208–235. <https://doi.org/10.1016/j.lithos.2014.06.012>
- Le Van De, 1997. Outline of Plate-Tectonic Evolution of Continental Crust of Vietnam. In: Dheeradilok, P., ed., Proceedings of the International Conferences on Stratigraphy and Tectonic Evolution of Southeast Asia and the South Pacific, Department of Mineral Resources, Bangkok, Thailand.
- Lepvrier, C., Faure, M., Van, N., et al., 2011. North-Directed Triassic Nappes in Northeastern Vietnam (East Bac Bo). *Journal of Asian Earth Sciences*, 41(1): 56–68. <https://doi.org/10.1016/j.jseas.2011.01.002>
- Lepvrier, C., Maluski, H., Van Tich, V., et al., 2004. The Early Triassic Indosinian Orogeny in Vietnam (Truong Son Belt and Kontum Massif); Implications for the Geodynamic Evolution of Indochina. *Tectonophysics*, 393(1/2/3/4): 87–118. <https://doi.org/10.1016/j.tecto.2004.07.030>
- Lepvrier, C., Maluski, H., Van Vuong, N., et al., 1997. Indosinian NW-Trending Shear Zones within the Truong Son Belt (Vietnam) <sup>40</sup>Ar–<sup>39</sup>Ar Triassic Ages and Cretaceous to Cenozoic Overprints. *Tectonophysics*, 283(1–4): 105–127. [https://doi.org/10.1016/s0040-1951\(97\)00151-0](https://doi.org/10.1016/s0040-1951(97)00151-0)
- Lepvrier, C., Van Vuong, N., Maluski, H., et al., 2008. Indosinian Tectonics in Vietnam. *Comptes Rendus Geoscience*, 340(2/3): 94–111. <https://doi.org/10.1016/j.crte.2007.10.005>
- Li, M. Z., Wu, C. L., Wu, D., et al., 2020. Geochemical and Zircon Hf Isotopic Characteristics of Mesozoic Intermediate-Acid Intrusive Rocks in Shuijadian Area, Tongling and Their Geological Significance. *Earth Science*, 45(7): 2555–2570 (in Chinese with English abstract).
- Li, X. H., Li, Z. X., Li, W. X., et al., 2007. U-Pb Zircon, Geochemical and Sr-Nd-Hf Isotopic Constraints on Age and Origin of Jurassic I- and A-Type Granites from Central Guangdong, SE China: A Major Igneous Event in Response to Foundering of a Subducted Flat-Slab? *Lithos*,

- os*, 96(1–2): 186–204. <https://doi.org/10.1016/j.lithos.2006.09.018>
- Li, X.Z., Liu, C.J. Ding, J., 2004. Correlation and Connection of the Main Suture Zones in the Greater Mekong Subregion. *Sedimentary Geology and Tethyan Geology*, 24(4): 1–12(in Chinese with English abstract).
- Liu, J. L., Tran, M. D., Tang, Y., et al., 2012. Permo-Triassic Granitoids in the Northern Part of the Truong Son Belt, NW Vietnam: Geochronology, Geochemistry and Tectonic Implications. *Gondwana Research*, 22(2): 628–644. <https://doi.org/10.1016/j.gr.2011.10.011>
- Luan, X.W., Wang, J., Liu, H., et al., 2021. A Discussion on Tethys in Northern Margin of South China Sea. *Earth Science*, 46(3): 866–884(in Chinese with English abstract).
- Ludwig, K. R., 2003. Isoplot/Ex, a Geochronological Toolkit for Microsoft Excel, Version 3.00. Berkeley Geochronology Center, Berkeley.
- Maluski, H., Lepvrier, C., Leyreloup, A., et al., 2005.  $^{40}\text{Ar}$ – $^{39}\text{Ar}$  Geochronology of the Charnockites and Granulites of the Kan Nack Complex, Kon Tum Massif, Vietnam. *Journal of Asian Earth Sciences*, 25(4): 653–677. <https://doi.org/10.1016/j.jseas.2004.07.004>
- Manaka, T., Zaw, K., Meffre, S., et al., 2014. The Ban Houayxai Epithermal Au–Ag Deposit in the Northern Lao PDR: Mineralization Related to the Early Permian Arc Magmatism of the Truong Son Fold Belt. *Gondwana Research*, 26(1): 185–197. <https://doi.org/10.1016/j.gr.2013.08.024>
- Marjorie, W., 1993. Magmatic Differentiation. *Journal of Geological Society*, 150(4): 611–624.
- Metcalfe, I., 1996. Gondwanaland Dispersion, Asian Accretion and Evolution of Eastern Tethys. *Australian Journal of Earth Sciences*, 43(6): 605–623. <https://doi.org/10.1080/08120099608728282>
- Metcalfe, I., 1998. Palaeozoic and Mesozoic Geological Evolution of the SE Asian Region: Multidisciplinary Constraints and Implications for Biogeography. *Biogeography and Geological Evolution of SE Asia*. Backhuys Publishers, Amsterdam, Netherlands, 25–41.
- Metcalfe, I., 2006. Palaeozoic and Mesozoic Tectonic Evolution and Palaeogeography of East Asian Crustal Fragments: The Korean Peninsula in Context. *Gondwana Research*, 9(1/2): 24–46. <https://doi.org/10.1016/j.gr.2005.04.002>
- Metcalfe, I., 2011. Tectonic Framework and Phanerozoic Evolution of Sundaland. *Gondwana Research*, 19(1): 3–21. <https://doi.org/10.1016/j.gr.2010.02.016>
- Metcalfe, I., 2013. Gondwana Dispersion and Asian Accretion: Tectonic and Palaeogeographic Evolution of Eastern Tethys. *Journal of Asian Earth Sciences*, 66(8): 1–33. <https://doi.org/10.1016/j.jseas.2012.12.020>
- Metcalfe, I., 2017. Tectonic Evolution of Sundaland. *Bulletin of the Geological Society of Malaysia*, 63: 27–60. <https://doi.org/10.7186/bgsm63201702>
- Metcalfe, I., 2021. Multiple Tethyan Ocean Basins and Orogenic Belts in Asia. *Gondwana Research*, 100: 87–130. <https://doi.org/10.1016/j.gr.2021.01.012>
- Minh, N. T., Dung, N. T., Hung, D. D., et al., 2020. Zircon U–Pb Ages, Geochemistry and Isotopic Characteristics of the Chu Lai Granitic Pluton in the Kontum Massif, Central Vietnam. *Mineralogy and Petrology*, 114(4): 289–303. <https://doi.org/10.1007/s00710-020-00707-x>
- Nagy, E. A., Maluski, H., Lepvrier, C., et al., 2001. Geodynamic Significance of the Kontum Massif in Central Vietnam: Composite  $^{40}\text{Ar}$ – $^{39}\text{Ar}$  and U–Pb Ages from Palaeozoic to Triassic. *The Journal of Geology*, 109(6): 755–770. <https://doi.org/10.1086/323193>
- Nakano, N., Osanai, Y., Minh, N. T., et al., 2008. Discovery of High-Pressure Granulite–Facies Metamorphism in Northern Vietnam: Constraints on the Permo-Triassic Indochinese Continental Collision Tectonics. *Comptes Rendus Geoscience*, 340(2/3): 127–138. <https://doi.org/10.1016/j.crte.2007.10.013>
- Nakano, N., Osanai, Y., Owada, M., et al., 2013. Tectonic Evolution of High-Grade Metamorphic Terranes in Central Vietnam: Constraints from Large-Scale Monazite Geochronology. *Journal of Asian Earth Sciences*, 73: 520–539. <https://doi.org/10.1016/j.jseas.2013.05.010>
- Nakano, N., Osanai, Y., Owada, M., et al., 2007. Geologic and Metamorphic Evolution of the Basement Complexes in the Kontum Massif, Central Vietnam. *Gondwana Research*, 12(4): 438–453. <https://doi.org/10.1016/j.gr.2007.01.003>
- Nakano, N., Osanai, Y., Owada, M., et al., 2021. Evolution of the Indochina Block from Its Formation to Amalgamation with Asia: Constraints from Protoliths in the Kontum Massif, Vietnam. *Gondwana Research*, 90: 47–62. <https://doi.org/10.1016/j.gr.2020.11.002>
- Nakano, N., Osanai, Y., Sajeev, K., et al., 2010. Triassic Eclogite from Northern Vietnam: Inferences and Geological Significance. *Journal of Metamorphic Geology*, 28(1): 59–76. <https://doi.org/10.1111/j.1525-1314.2009.00853.x>

- Nguyen, Q. M., Feng, Q., Zi, J. W., et al., 2019. Cambrian Intra-Oceanic Arc Trondhjemite and Tonalite in the Tam Ky-Phuoc Son Suture Zone, Central Vietnam: Implications for the Early Paleozoic Assembly of the Indochina Block. *Gondwana Research*, 70: 151–170. <https://doi.org/10.1016/j.gr.2019.01.002>
- Nguyen, T. T. B., Satir, M., Siebel, W., et al., 2004. Granitoids in the Dalat Zone, Southern Vietnam: Age Constraints on Magmatism and Regional Geological Implications. *International Journal of Earth Sciences*, 93(3): 329–340. <https://doi.org/10.1007/s00531-004-0387-6>
- Osanai, Y., Nakano, N., Owada, M., et al., 2004. Permo-Triassic Ultrahigh-Temperature Metamorphism in the Kontum Massif, Central Vietnam. *Journal of Mineralogical and Petrological Sciences*, 99(4): 225–241. <https://doi.org/10.2465/jmps.99.225>
- Osanai, Y., Nakano, N., Owada, M., et al., 2008. Collision Zone Metamorphism in Vietnam and Adjacent South-Eastern Asia: Proposition for Trans Vietnam Orogenic Belt. *Journal of Mineralogical and Petrological Sciences*, 103(4): 226–241. <https://doi.org/10.2465/jmps.080620e>
- Owada, M., Osanai, Y., Hokada, T., et al., 2006. Timing of Metamorphism and Formation of Garnet Granite in the Kontum Massif, Central Vietnam: Evidence from Monazite EMP Dating. *Journal of Mineralogical and Petrological Sciences*, 101(6): 324–328. <https://doi.org/10.2465/jmps.060617a>
- Owada, M., Osanai, Y., Nakano, N., et al., 2007. Crustal Anatexis and Formation of Two Types of Granitic Magmas in the Kontum Massif, Central Vietnam: Implications for Magma Processes in Collision Zones. *Gondwana Research*, 12(4): 428–437. <https://doi.org/10.1016/j.gr.2006.11.001>
- Owada, M., Osanai, Y., Nakano, N., et al., 2016. Late Permian Plume-Related Magmatism and Tectonothermal Events in the Kontum Massif, Central Vietnam. *Journal of Mineralogical and Petrological Sciences*, 111(3): 181–195. <https://doi.org/10.2465/jmps.151019b>
- Owada, M., Osanai, Y., Nakano, N., et al., 2020. Timing of Magmatism and Ultrahigh- to High-Grade Metamorphism in the Kannak Complex, Kon Tum Massif, Vietnam: Magmatic Activity and Its Tectonic Implications. *Journal of Asian Earth Sciences*, 200: 104077. <https://doi.org/10.1016/j.jseas.2019.104077>
- Patino Douce, A. E., 1999. What do Experiments Tell Us about the Relative Contributions of Crust and Mantle to the Origin of Granitic Magmas? *Geological Society, London, Special Publications*, 168(1): 55–75. <https://doi.org/10.1144/gsl.sp.1999.168.01.05>
- Patino Douce, A. E., Harris, N., 1998. Experimental Constraints on Himalayan Anatexis. *Journal of Petrology*, 39(4): 689–710. <https://doi.org/10.1093/petroj/39.4.689>
- Pearce, J. A., 1996. Sources and Settings of Granitic Rocks. *Episodes*, 19(4): 120–125. <https://doi.org/10.18814/epiugs/1996/v19i4/005>
- Pham, M., Hieu, P. T., Hoang, N. K., 2018. Geochemical and Geochronological Studies of the Muong Hum Alkaline Granitic Pluton from the Phan Si Pan Zone, Northwest Vietnam: Implications for Petrogenesis and Tectonic Setting. *Island Arc*, 27(4): e12250. <https://doi.org/10.1111/iar.12250>
- Qian, X., Feng, Q. L., Wang, Y. J., et al., 2016a. Petrochemistry and Tectonic Setting of the Middle Triassic Arc-Like Volcanic Rocks in the Sayabouli Area, NW Laos. *Journal of Earth Science*, 27(3): 365–377. <https://doi.org/10.1007/s12583-016-0669-5>
- Qian, X., Feng, Q. L., Wang, Y. J., et al., 2016b. Geochronological and Geochemical Constraints on the Mafic Rocks along the Luang Prabang Zone: Carboniferous Back-Arc Setting in Northwest Laos. *Lithos*, 245(16): 60–75. <https://doi.org/10.1016/j.lithos.2015.07.019>
- Qian, X., Feng, Q. L., Wang, Y. J., et al., 2016c. Geochronological and Geochemical Constraints on the Origin of the Meta-Basic Volcanic Rocks in the Tengtiaohe Zone, Southeast Yunnan. *Acta Geologica Sinica*, 90(2): 669–683. <https://doi.org/10.1111/1755-6724.12697>
- Qian, X., Li, H. L., Yu, X. Q., et al., 2022. Permian-Triassic Magmatism along the Truong Son Zone in SE Asia and Its Paleotethyan Tectonic Implications. *Geotectonica et Metallogenesis*, 46(3): 585–604(in Chinese with English abstract).
- Qian, X., Wang, Y. J., Zhang, Y. Z., et al., 2019. Petrogenesis of Permian-Triassic Felsic Igneous Rocks along the Truong Son Zone in Northern Laos and Their Paleotethyan Assembly. *Lithos*, 328/329: 101–114. <https://doi.org/10.1016/j.lithos.2019.01.006>
- Qian, X., Wang, Y. J., Zhang, Y. Z., et al., 2020. Late Triassic Post-Collisional Granites Related to Paleotethyan Evolution in Northwestern Lao PDR: Geochronological and Geochemical Evidence. *Gondwana Research*, 84: 163–176. <https://doi.org/10.1016/j.gr.2020.03.002>
- Roger, F., Jolivet, M., Maluski, H., et al., 2014. Emplacement and Cooling of the Dien Bien Phu Granitic Com-

- plex: Implications for the Tectonic Evolution of the Dien Bien Phu Fault (Truong Son Belt, NW Vietnam). *Gondwana Research*, 26(2): 785–801. <https://doi.org/10.1016/j.gr.2013.07.018>
- Sang, D. Q., 2011. Petrographic Characteristics and Zircon U-Pb Geochronology of Granitoid Rocks in the Southern Ben Giang, Quang Nam. *SciTech Development*, 14: 17–30(in Vietnamese with English abstract).
- Shellnutt, J. G., Lan, C. Y., Van Long, T., et al., 2013. Formation of Cretaceous Cordilleran and Post-Orogenic Granites and Their Microgranular Enclaves from the Dalat Zone, Southern Vietnam: Tectonic Implications for the Evolution of Southeast Asia. *Lithos*, 182/183: 229–241. <https://doi.org/10.1016/j.lithos.2013.09.016>
- Shi, M. F., Lin, F. C., Fan, W. Y., et al., 2015. Zircon U-Pb Ages and Geochemistry of Granitoids in the Truong Son Terrane, Vietnam: Tectonic and Metallogenic Implications. *Journal of Asian Earth Sciences*, 101(1): 101–120. <https://doi.org/10.1016/j.jseas.2015.02.001>
- Shi, M. F., Lin, F. C., Li, X. Z., et al., 2011. Stratigraphic Zoning and Tectonic Events in Indochina and Adjacent Areas of Southwest China. *Geology in China*, 38(5): 1244–1256(Chinese with English abstract).
- Söderlund, U., Patchett, P. J., Vervoort, J. D., et al., 2004. The  $^{176}\text{Lu}$  Decay Constant Determined by Lu-Hf and U-Pb Isotope Systematics of Precambrian Mafic Intrusions. *Earth and Planetary Science Letters*, 219(3–4): 311–324. [https://doi.org/10.1016/S0012-821X\(04\)00012-3](https://doi.org/10.1016/S0012-821X(04)00012-3)
- Sone, M., Metcalfe, I., 2008. Parallel Tethyan Sutures in Mainland Southeast Asia: New Insights for Palaeo-Tethys Closure and Implications for the Indosian Orogeny. *Comptes Rendus Geoscience*, 340(2–3): 166–179. <https://doi.org/10.1016/j.crte.2007.09.008>
- Sun, S. S., McDonough, W. F., 1989. Chemical and Isotopic Systematics of Oceanic Basalts: Implications for Mantle Composition and Processes. *Geological Society, London, Special Publications*, 42(1): 313–345. <https://doi.org/10.1144/gsl.sp.1989.042.01.19>
- Sylvester, P. J., 1989. Post-Collisional Alkaline Granites. *The Journal of Geology*, 97(3): 261–280. <https://doi.org/10.1086/629302>
- Sylvester, P. J., 1998. Post-Collisional Strongly Peraluminous Granites. *Lithos*, 45(1–4): 29–44. [https://doi.org/10.1016/S0024-4937\(98\)00024-3](https://doi.org/10.1016/S0024-4937(98)00024-3)
- Tao, J.H., Li, W.X., Li, X.H., et al., 2013. Geochronology, Geochemistry and Zircon Hf-O Isotope of Yanshanian High Heteromorphism Granite in Long Yuan Ba Area, South Jiangxi Province. *Scientia Sinica (Terra)*, 43(5): 770–788 (in Chinese).
- Thanh, N. X., Hai, T. T., Hoang, N., et al., 2014. Back-arc Mafic-Ultramafic Magmatism in Northeastern Vietnam and Its Regional Tectonic Significance. *Journal of Asian Earth Sciences*, 90: 45–60. <https://doi.org/10.1016/j.jseas.2014.04.001>
- Thuc, D. D., Trung, H., 1995. Vietnam Geology, Part of II: Magma. Science and Technics Publishing House, HaNoi, 359.
- Tinh, N. X., Pham, M., Do, N. T. H., et al., 2021. Zircon U-Pb Isotope Age and Hf Isotope Composition of the Ea H'Leo Granite in Dak Lak Area. *Science Technology Development Journal—Science of the Earth Environment*, 5: 200–211.
- Tran, H. T., Zaw, K., Halpin, J. A., et al., 2014. The Tam Ky-Phuoc Son Shear Zone in Central Vietnam: Tectonic and Metallogenic Implications. *Gondwana Research*, 26(1): 144–164. <https://doi.org/10.1016/j.gr.2013.04.008>
- Tran, N. N., 1998. Thermotectonic Events from Early Proterozoic to Miocene in the Indochina Craton: Implication of K-Ar Ages in Vietnam. *Journal of Asian Earth Sciences*, 16(5/6): 475–484. [https://doi.org/10.1016/S0743-9547\(98\)00027-0](https://doi.org/10.1016/S0743-9547(98)00027-0)
- Tri, T. V., Khuc, V., 2011. Geology and Earth Resources of Vietnam. Publishing House for Science and Technology, HaNoi, 634.
- Trong, N. H., Zong, K. Q., Liu, Y. S., et al., 2021. Early Paleozoic Arc Magmatism and Accretionary Orogenesis in the Indochina Block, Southeast Asia. *The Journal of Geology*, 129(1): 33–48. <https://doi.org/10.1086/713727>
- Usuki, T., Lan, C. Y., Yui, T. F., et al., 2009. Early Paleozoic Medium-Pressure Metamorphism in Central Vietnam: Evidence from SHRIMP U-Pb Zircon Ages. *Geosciences Journal*, 13(3): 245–256. <https://doi.org/10.1007/s12303-009-0024-2>
- van Thanh, T., Hieu, P. T., Minh, P., et al., 2019. Late Permian-Triassic Granitic Rocks of Vietnam: The Muong Lat Example. *International Geology Review*, 61(15): 1823–1841. <https://doi.org/10.1080/00206814.2018.1561335>
- Wakita, K., Metcalfe, I., 2005. Ocean Plate Stratigraphy in East and Southeast Asia. *Journal of Asian Earth Sciences*, 24(6): 679–702. <https://doi.org/10.1016/j.jseas.2004.04.004>
- Wang, H., Lin, F. C., Li, X. Z., et al., 2015. The Division

- of Tectonic Units and Tectonic Evolution in Laos and Its Adjacent Regions. *Geology in China*, 42(1): 71—84 (in Chinese with English abstract).
- Wang, S. F., Mo, Y., Wang, C., et al., 2016a. Paleotethyan Evolution of the Indochina Block as Deduced from Granites in Northern Laos. *Gondwana Research*, 38: 183—196.
- Wang, Y. J., He, H. Y., Cawood, P. A., et al., 2016b. Geochronological, Elemental and Sr-Nd-Hf-O Isotopic Constraints on the Petrogenesis of the Triassic Post-Collisional Granitic Rocks in NW Thailand and Its Paleotethyan Implications. *Lithos*, 266/267: 264—286. <https://doi.org/10.1016/j.lithos.2016.09.012>
- Wang, Y. J., Zhou, Y., Cai, Y. F., 2016c. Geochronological and Geochemical Constraints on the Petrogenesis of the Ailaoshan Granitic and Migmatite Rocks and Its Implications on Neoproterozoic Subduction along the SW Yangtze Block. *Precambrian Research*, 283: 106—124. <https://doi.org/10.1016/j.precamres.2016.07.017>
- Wang, Y. J., Qian, X., Cawood, P. A., et al., 2018. Closure of the East Paleotethyan Ocean and Amalgamation of the Eastern Cimmerian and Southeast Asia Continental Fragments. *Earth-Science Reviews*, 186: 195—230. <https://doi.org/10.1016/j.earscirev.2017.09.013>
- Wang, Y. J., Qian, X., Cawood, P. A., et al., 2021. Prototethyan Accretionary Orogenesis along the East Gondwana Periphery: New Insights from the Early Paleozoic Igneous and Sedimentary Rocks in the Sibumasu. *Geochemistry, Geophysics, Geosystems*, 22(5): e2020GC009622. <https://doi.org/10.1029/2020GC009622>
- Wang, Y. J., Yang, T. X., Zhang, Y. Z., et al., 2020. Late Paleozoic Back-Arc Basin in the Indochina Block: Constraints from the Mafic Rocks in the Nan and Luang Prabang Tectonic Zones, Southeast Asia. *Journal of Asian Earth Sciences*, 195(15): 104333. <https://doi.org/10.1016/j.jseas.2020.104333>
- Whalen, J. B., Currie, K. L., Chappell, B. W., 1987. A-Type Granites: Geochemical Characteristics, Discrimination and Petrogenesis. *Contributions to Mineralogy and Petrology*, 95(4): 407—419. <https://doi.org/10.1007/BF00422022>
- Wiedenbeck, M., Allé, P., Corfu, F., et al., 1995. Three Natural Zircon Standards for U-Th-Pb, Lu-Hf, Trace Element and REE Analyses. *Geostandards Newsletter*, 19(1): 1—23. <https://doi.org/10.1111/j.1751-908X.1995.tb00147.x>
- Winchester, J. A., Floyd, P. A., 1977. Geochemical Discrimination of Different Magma Series and Their Differentiation Products Using Immobile Elements. *Chemical Geology*, 20(4): 325—343. [https://doi.org/10.1016/0009-2541\(77\)90057-2](https://doi.org/10.1016/0009-2541(77)90057-2)
- Wu, F. Y., Liu, X. C., Ji, W. Q., et al., 2017. Highly Fractionated Granites: Recognition and Research. *Scientia Sinica (Terra)*, 47(7): 745—765 (in Chinese).
- Wu, S. Y., Nie, F., Liu, S. S., et al., 2022. The Discovery of Ophiolitic Complex in Namhonr, Northern Loei Tectonic Belt and Its Geological Significance. *Earth Science*, 47(8): 2871—2888 (in Chinese with English abstract).
- Wu, Y. B., Zheng, Y. F., 2004. Genetic Mineralogy of Zircon and Its Constraints on U-Pb Age Interpretation. *Chinese Science Bulletin*, 49(16): 1589—1604 (in Chinese).
- Xu, C., Gan, C. S., Hieu, P. T., et al., 2022. Geochronology and Geochemistry of Mesoproterozoic Mafic Rocks in the Kontum Complex and Its Implication for the Columbia Reconstruction. *Lithosphere*, 4967935. <https://doi.org/10.2113/2022/4967935>
- Xu, C., Wang, Y. J., Qian, X., et al., 2020. Geochronological and Geochemical Characteristics of Early Silurian S-Type Granitic Gneiss in Takengon Area of Northern Sumatra and Its Tectonic Implications. *Earth Science*, 45(6): 2077—2090 (in Chinese with English abstract).
- Yang, J. S., Xu, Z. Q., Li, T. F., et al., 2007. Oceanic Subduction-Type Eclogite in the Lhasa Block, Tibet, China: Remains of the Paleo-Tethys Ocean Basin? *Geological Bulletin of China*, 26(10): 1277—1287.
- Yang, W. Q., Qian, X., Feng, Q. L., et al., 2016. Zircon U-Pb Geochronological Evidence for the Evolution of the Nan-Uttaradit Suture in Northern Thailand. *Journal of Earth Science*, 27(3): 378—390. <https://doi.org/10.1007/s12583-016-0670-z>
- Yu, X. Q., Qian, X., Zhang, Y. Z., et al., 2021. Geochemical Characteristics of the Early Eocene S-Type Granites in Panti, Central Sumatra and Its Neotethyan Tectonic Implications. *Geotectonica et Metallogenesis*, 45(3): 570—585 (in Chinese with English abstract).
- Zhang, R. Y., Lo, C. H., Chung, S. L., et al., 2013. Origin and Tectonic Implication of Ophiolite and Eclogite in the Song Ma Suture Zone between the South China and Indochina Blocks. *Journal of Metamorphic Geology*, 31(1): 49—62. <https://doi.org/10.1111/jmg.12012>
- Zhang, R. Y., Lo, C. H., Li, X. H., et al., 2014. U-Pb Dating and Tectonic Implication of Ophiolite and Metabasite from the Song Ma Suture Zone, Northern Vietnam. *American Journal of Science*, 314(2): 649—678. <https://doi.org/10.2475/02.2014.07>
- Zhang, Y. Z., Yang, X., Wang, Y. J., et al., 2020. Rifting

- and Subduction Records of the Paleo-Tethys in North Laos: Constraints from Late Paleozoic Mafic and Plagiogranitic Magmatism along the Song Ma Tectonic Zone. *Geological Society of America Bulletin*, 133(1–2): 212–232.
- Zhang, Z. W., Shu, Q., Yang, X. Y., et al., 2019. Review on the Tectonic Terranes Associated with Metallogenic Zones in Southeast Asia. *Journal of Earth Science*, 30(1): 1–19.
- Zhao, G.F., Liu, H.C., Qian, X., et al., 2018. Petrogenesis of Late Permian I -Type Granites in SE Hainan Island and Its Tectonic Implication for Paleotethyan Evolution. *Earth Science*, 43(4): 1321–1332(in Chinese with English abstract).
- Zhao, T. Y., Qian, X., Feng, Q. L., 2016. Geochemistry, Zircon U-Pb Age and Hf Isotopic Constraints on the Petrogenesis of the Silurian Rhyolites in the Loei Fold Belt and Their Tectonic Implications. *Journal of Earth Science*, 27(3): 391–402.
- Zheng, Y. F., 2021. Metamorphism in Subduction Zones. *Reference Module in Earth Systems and Environmental Sciences*.
- Zi, J. W., Cawood, P. A., Fan, W. M., 2012a. Generation of Early Indosinian Enriched Mantle-Derived Granitoid Pluton in the Sanjiang Orogen (SW China) in Response to Closure of the Paleo-Tethys. *Lithos*, 140/141: 166–182. <https://doi.org/10.1016/j.lithos.2012.02.006>
- Zi, J. W., Cawood, P. A., Fan, W. M., et al., 2012b. Contrasting Rift and Subduction-Related Plagiogranites in the Jinshajiang Ophiolitic Mélange, Southwest China, and Implications for the Paleo-Tethys. *Tectonics*, 31(2): TC2012. <https://doi.org/10.1029/2011tc002937>
- 矿作用. 北京: 地质出版社.
- 李名则, 吴才来, 吴迪, 等, 2020. 铜陵舒家店地区中生代中酸性侵入岩锆石 Hf 同位素特征及其地质意义. *地球科学*, 45(7): 2555–2570.
- 李兴振, 刘朝基, 丁俊, 2004. 大湄公河次地区主要结合带的对比与连接. *沉积与特提斯地质*, 24(4): 1–12.
- 栾锡武, 王嘉, 刘鸿, 等, 2021. 关于南海北部特提斯的讨论. *地球科学*, 46(3): 866–884.
- 钱鑫, 李慧玲, 余小清, 等, 2022. 东南亚长山构造带二叠纪—三叠纪岩浆作用及其古特提斯构造意义. *大地构造与成矿学*, 46(3): 585–604.
- 施美凤, 林方成, 李兴振, 等, 2011. 东南亚中南半岛与中国西南邻区地层分区及沉积演化历史. *中国地质*, 38(5): 1244–1256.
- 陶继华, 李武显, 李献华, 等, 2013. 赣南龙源坝地区燕山期高分异花岗岩年代学、地球化学及锆石 Hf-O 同位素研究. *中国科学: 地球科学*, 43(5): 770–788.
- 王宏, 林方成, 李兴振, 等, 2015. 老挝及邻区构造单元划分与构造演化. *中国地质*, 42(1): 71–84.
- 吴福元, 刘小驰, 纪伟强, 等, 2017. 高分异花岗岩的识别与研究. *中国科学: 地球科学*, 47(7): 745–765.
- 吴松洋, 聂飞, 刘书生, 等, 2022. 黎府构造带北部南莫溪蛇绿混杂岩的发现及其地质意义. *地球科学*, 47(8): 2871–2888.
- 吴元保, 郑永飞, 2004. 锆石成因矿物学研究及其对 U-Pb 年龄解释的制约. *科学通报*, 49(16): 1589–1604.
- 徐畅, 王岳军, 钱鑫, 等, 2020. 苏门答腊岛北部 Takengon 早志留世 S 型花岗片麻岩年代学、地球化学特征及构造意义. *地球科学*, (6): 2077–2090.
- 余小清, 钱鑫, 张玉芝, 等, 2021. 苏门答腊中部 Panti 早始新世 S 型花岗岩地球化学特征及其新特提斯构造意义. *大地构造与成矿学*, 45(3): 570–585.
- 赵国锋, 刘汇川, 钱鑫, 等, 2018. 琼东南晚二叠世 I 型花岗岩成因及其构造指示. *地球科学*, 43(4): 1321–1332.

## 附中文参考文献

邓晋福, 罗照华, 苏尚国, 等, 2004. 岩石成因、构造环境与成